# PERFORMANCE STUDIES OF CAVITY EXPANSOMETER

*A Thesis submitted*
*in partial fulfilment of the*
*requirements for the Degree of*
**MASTER OF TECHNOLOGY**



*by*

**DEVENDRA KUMAR**

to the
DEPARTMENT OF CIVIL ENGINEERING
INDIAN INSTITUTE OF TECHNOLOGY KANPUR

MAY, 1991

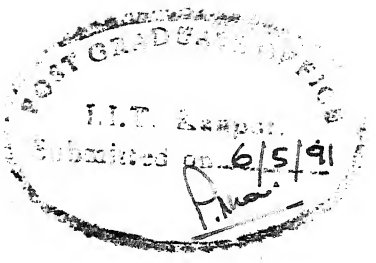


# CERTIFICATE

This is to certify that the thesis entitled, *"Performance Studies of Cavity Expansometer"* is a work carried out by Mr. *Devendra Kumar* under my supervision and that this work has not been submitted elsewhere for a degree.

( P. K. Basudhar )
Assistant Professor
Civil Engineering Department
Indian Institute of Technology Kanpur,
Kanpur - 208016

May 1991

# A C K N O W L E D G E M E N T

It is my great pleasure to express my gratitude and deep regard to Dr. P.K. Basudhar, my thesis supervisor, for his invaluable guidance, constant encouragement, immense co-operation and fruitful discussions throughout the study of the present work. He would never cease to be a source of inspiration for me.

Although, all my friends have helped me one way or the other. I owe a special debt to Atul Kumar, S.B. Pandey, Jayant Kumar, M.K. Chaturbedi, M.K. Jha, Sanjay Saxena for their help and encouragement.

I also wish to thank Geotechnical Laboratory Staffs,Mr. R.K. Trivedi, Mr. A.K. Srivastava, Mr. Gulab and Mr. Parsuram for their help at the various stages of the present work. The excellent typing by Mr. B.P. Pant and the excellent tracing by Mr. J.C. Verma are highly acknowledged.

The immense patience, sacrifices, encouragement and moral support of my brothers and father are greatly appreciated and remembered.

Devendra Kumar

# CONTENTS

# NOMENCLATURES

| | |
|---|---|
| DST | Direct Shear Test |
| E | Elastic Modulus |
| G | Shear Modulus |
| K | Bearing Capacity Factor |
| $K_o$ | Coefficient of Earth Pressure at Rest |
| $L_a$ | Effective Length of Probe |
| MPM | Me'nard Pressuremeter Test |
| N | Standard Penetration Number |
| PLT | Plate Load Test |
| PBP | Prebored Pressuremeter Test |
| $p_i$ | Internal Pressure |
| $p_l$ | Limit Pressure |
| $p_o$ | Total Insitu Horizontal Earth Pressure |
| $q_l$ | Ultimate Base Resistance |
| $q_c$ | Cone Resistance |
| R | Radius of the Tube |
| SCPT | Static Cone Penetration Test |
| SPT | Standard Penetration Test |
| $V_c$ | Corrected Volume of the Probe |
| $V_f$ | Volume of the fluid injected |
| $V_n$ | Normal Volume of the Probe |
| $V_t$ | Theoretical Volume of the Probe |
| $\epsilon_v$ | Volumetric Strain |
| $\epsilon_\theta$ | Circumferential Strain |
| $\nu$ | Poisson's Ratio |
| f | An Emperical Co-efficient which is a Function of Soil and Geometry of the Footing |
| $\phi'$ | Angle of Shearing Resistance |
| $q_l$ | Ultimate Base Resistance |
| $q^*$ | Net base resistance |

# LIST OF FIGURES

# LIST OF TABLES

# ABSTRACT

The thesis pertains to study of reliability of cavity expansometer : a monocell pressuremeter. The investigation has been conducted in two phases. First studies have been made to find the behaviour of the probe under free air and restrained expansion condition. The free air expansion technique is the standard method of calibrating pressuremeters where as the restrained expansion technique is the improved calibration method. This study brings out the difference between the two calibration procedures. The deformed shape of the probe has also been studied by developing a very simple and cheap technique than using the standard x-ray radiography method. Lastly the performance of the cavity expansometer in predicting soil parameters, foundation settlement and bearing capacity has also been examined by comparing the obtained results with the results obtained from other field tests like static cone penetration test, plate load test, laboratory test data and standard co-relations available in literature.

It has been observed that the central portion of the probe expand uniformly indicating a very good choice of l/d ratio. It has also been observed that over the central portion the pressure distribution is more or less uniform.

The predictions regarding the soil parameters, bearing capacity and settlement of footing on sand using cavity expansometer compares very well with those predicted from the data obtained from static cone penetration test and plate load test. On the whole it has been observed that the performance of cavity expansometer is excellent.

# 1. INTRODUCTION

## 1.1 General :

It is well recognised that laboratory methods of soil testing are inadequate due to disturbance of soil structure during sampling, stress release and change in pore water pressure, during subsequent storage and impossibility of obtaining representative samples in certain type of soils.

To circumvent the above short-coming of laboratory tests, over the years, several in-situ tests have been developed. Some of the commonly used tests are

i) Standard Penetration Test (SPT)

ii) Static and Dynamic Cone Penetration Test (SCPT, DCPT)

iii) Vane Shear Test (VST)

iv) Plate Load Test (PLT)

v) Pressuremeter Test (PMT)

vi) Dilatometer Test (DMT)

Out of these tests SPT, SCPT, DCPT, VST measure the parameters at the ultimate or failure state only and give no idea about the stress-strain relationship of soil before failure. Plate load test is considered superior to other in-situ methods but it is very costly and can only be performed at shallow depths in limited numbers. These factors led to development of Pressuremeter and Dilatometer, which can be used to carry out large number of in-situ, truly static load test at greater depths. The advantages of these tests over the other in-situ tests have been reported in literature.

## 1.2 History of Development of Pressuremeter :

Kögler (1933) first proposed the idea of expanding bore hole wall with the help of balloon like device in order to measure the stress-strain response of soil. However, his work went more or less unnoticed. In 1955 Louis Menard revived the idea proposed by Kögler and introduced a major change in the design of the probe. The test procedure and interpretation methods are standardised for Menard pressuremeter (MPM) and design methods based on empirical relationships are available for the design of foundations (Baguelin et al. 1978, Mair and Wood, 1987).

As the pressuremeter testing gained more and more acceptance several equipment, often differing from MPM with respect to the probe dimensions and configuration, mode of operation and measurement system were built in Japan, Canada, Australia, and United Kingdom. A pressuremeter called lateral load tester (LLT) was developed by OYO corporation of Japan. The equipment is of moderate capacity (5000 kpa). The same company developed a high capacity device (20,000 kpa) named `Elastmeter'. Both the equipments have monocell probe. Elastmeter contains displacement detecting mechanism to measure the diameter of the bore hole at any stage of test and thus eliminates the requirement of volume measurement. A Similar mechanism has also been used in COFFEY PMX-20 developed in Australia 1978. All the equipments mentioned above are stress controlled.

In order to try and over come the problem of disturbance in conventional pressuremeter test (MPM), the concept of self boaring pressuremeter have been developed both in United Kingdom

(Wroth and Hughes 1973) and France (Baguelin et al. 1972). For reliable measurement of the in-situ properties of stiff clays, the push-in-pressuremeter (PIP) was developed in U.K. (Henderson et al. 1979). Till 1979 pressuremeter was not manufactured in India. S. Venkatesan of Central Building Research Institute of Roorkee in collaboration with M/s Associated Instrument Manufacturers Ltd. of New Delhi undertook the development of what is now known as subsoil deformeter (Venkatesan, 1980).

The pressuremeters available to Geo-technical engineers are highly sophisticated instrument. Because of this, skilled persons are required for its handling. The equipment is highly under used in underdeveloped and developing countries partly due to lack of skilled man power and mainly due to the high cost of the equipment. Because of this efforts have been made to develop simplified pressuremeter devices.

Strain controlled simplified pressuremeter apparatus called the Texam pressuremeter has been developed by M/s Rocktest of Canada (Capelle, 1983). However, the credit for building the first strain controlled equipment goes to Bission and Marigner in France (Baguelin et al. 1978). A manually operated, strain controlled, monocell pressuremeter called cavity expansometer (Cavitex) have been developed at I I T Kanpur (Chauhan 1989) retaining all the inherent advantages of pressuremeter technique and keeping in view the simplicity of design, operation and robustness of construction. Chauhan and Basudhar (1989) estimated the pressure loss due to the expansion of rubber membrane and covering overlapping steel strips using free air expansion technique. Murat and Lemoigne (1988) emphasised the importance of

an improved calibration and correction technique for pressuremeter in relation with membrane reaction highlighting the difference between unrestrained and confined inflation test. As such there is a need of improved calibration as suggested by them to recalibrate the Cavitex.

## 1.3 Interpretation of Test Results :

### 1.3.1 General :

Once the corrections are applied to the data obtained from a properly conducted pressuremeter test, various soil properties can be determined using various theories. Pressuremeter tests can be used to estimate the value of shear modulus, in-situ total horizontal stress, angle of shearing resistance and dilation for sand deposits etc. The analytical procedures as available in the literature are presented briefly as follows :

### 1.3.2 Determination of angle of shearing resistance ($\phi$') :

Gibson and Anderson (1961) interpreted data of pressuremeter tests in sandy soils assuming that sand behaved perfectly elastically until failure and that the sand continued to fail at constant ratio of effective stresses and at constant volume. Their analysis related the applied effective pressure $\sigma_{ra}$' with the volumetric strain of the pressuremeter $(\frac{\Delta V}{V_o})$ by the following expression:

$$\sigma_{ra}' = \left(\frac{2\sigma_{ro}'}{1+N}\right)\left[\left(\frac{E}{2\sigma_{ro}'(1+N)}\right)\left(\frac{1+N}{1-N}\right)\left(\frac{\Delta V}{V}\right)\right]^{\frac{1-N}{2}} \qquad (1.1)$$

Hence the value of N can be determined by plotting log $\sigma_{ra}'$ against log $(\frac{\Delta V}{V})$ and measuring the gradient of the resulting straight line which is equal $\frac{1}{2}$ (1-N) or $\frac{\sin \phi'}{1+\sin\phi}$. The major flaw in this analysis is the assumption that at failure the sand deformes at constant volume. This method assumes that no volume change occur during the deformation, which is unrealistic. It underestimate the value of $\phi'$ when the sand is compacting and over-estimate the value when sand is dilating.

### 1.3.3 Determination of Pressuremeter Modulus :

Over the linear portion of the pressure-volume curve the soil is said to behave as more or less elastic material. However, it should be appreciated that soil has no unique value of modulus and it is more appropriate to call this modulus as "pressuremeter modulus". The value of shear modulus `G' is obtained by equation for radial expansion of cylindrical cavity in an infinite elastic medium

$$G = v_o \left(\frac{\Delta p}{\Delta v}\right) \qquad (1.2)$$

To convert the shear modulus `G' to Young's modulus (E), again assuming that soil is elastic, the following well known relationship is used.

$$G = \frac{E}{2(1+\nu)} \qquad (1.3)$$

where $\nu$ is the Poisson's ratio of the soil.

### 1.3.4 Estimation of Earth pressure at rest ($p_o$) :

The total horizontal pressure in the ground before any drilling or testing starts should be estimated for each test elevation. Total stress is calculated from the equation

$$p_o = (Z\,\gamma - u)K_o + u \qquad (1.4)$$

where $Z$ is the depth below ground level, $\gamma$ is the total unit weight of soil; $K_o$ is the coefficient of earth pressure at rest; u is the pore water pressure at the level of the probe.

The standard method for estimating $p_o$ is to assume that it corresponds to the start of linear region of pressure-volume curve. $p_o$ is estimated by initial first kink of the pressuremeter curve. Since this is said to mark the moment when the wall of the hole were pushed back to the original position, the pressure in the probe at that stage is equal to total horizontal earth pressure at rest. There are two practical problems that arise in determining $p_o$.

a) There are too few points available at the start of the test to enable a precise curve to be drawn so that $p_o$ can be determined with any degree of accuracy.

b) If diameter of the hole is much larger than the diameter

of the probe, the resistance of membrane and sheath can be appreciable when compared with the small pressure required to reach $p_o$, this leads to considerable error.

There is evidence to suggest that the method underestimates $p_o$ in over consolidated soil by considerable amount.

### 1.3.5 Extrapolation for Limit pressure ($p_l$) :

Pressuremeter tests which are performed have limits on pressure and available water supply which may cause the test to be terminated prematurely in hard soil or rock. The limit on pressure are due to the risk of membrane brusting or damaging the internal organs of the control unit and the probe, the limits on water supply are due to the finite capacity of the cylinder and the probe. These physical limitations of the apparatus have a direct bearing on the experimental determination of the conventional limit pressure $p_l$. The simplest way to extrapolate the curve is to extend the curve smoothly till it reaches the point corresponding to double the original size of cavity. This method cannot be used when a test is terminated soon after the initial yield. The method that is generally adopted to determine the limit pressure is briefly presented as follows :

In this method the ordinate and abscissa in a log-log plot are respectively chosen as the corrected pressure (p) and the ratio of the increase in the volume of the cavity ($\Delta V$) to its initial volume ($v_o$). The straight line portion of the curve obtained is extended to find the limit pressure ($p_l$) corresponding

to the value of $\frac{\Delta v}{v_o} = 1$. This is an indirect way of finding the limit pressure at which the cavity volume often the expansion due to the applied pressure becomes double of its initial volume.

### 1.3.6 Bearing Capacity :

The following relationship can be used to compute ultimate base resistance of foundation.

$$q_l = q_o + K (p_l - p_o) \tag{1.5}$$

$$q^* = Kp_l^* \tag{1.6}$$

Where $q^* = q - q_o$ and $p_L^* = P_L - P_o$

where $q_o$ is computed from unit weight of soil, $p_o$ and $p_l$ from the pressuremeter test result. The bearing capacity factor 'K' is dependent on number of variables like type of soil, depth of foundation and foundation shape.

### 1.3.7 Settlement Analysis :

Menard is credited with suggesting a simple semi empirical formula to estimate the settlement (Baguelin et al. 1978)

$$s = \frac{q_{net}}{E_M} \times f \tag{1.7}$$

where $q_{net} = q - \gamma D$

f = an empirical co-efficient which is a function of nature of soil and geometry of footing. (Fig.1.1).

$E_M$ = Pressuremeter modulus which applies within a depth of 2B below the foundation

## 1.4 Motivation and Scope of the thesis :

When a new equipment is developed it is essential to check its performance in the field in various types of deposits. The performance of the cavity expansometer hereafter called Cavitex in clayey silt deposit was studied by Chauhan (1989). The obtained results, were compared with the results obtained by using SCPT and SPT. From the comparative studies Chauhan (1989) concluded that the performance of the Cavitex in predicting the nature of soil deposit at site and soil properties like elastic modulus (pressuremeter modulus) and undrained shear strength was reliable. However, no studies were made to find its performance in sand deposits.

As such, an effort has been made in this thesis to study the reliability of the Cavitex in sand. A comparative study to find the efficiency of different field tests like SPT, SCPT, PLT and PMT using Cavitex in predicting the bearing capacity and settlement of shallow foundations have been made and presented in order to establish the credential of the Cavitex with respect to the other field tests as mentioned.

In chapter two a brief description of the Cavity Expansometer (Cavitex) has been given.

In chapter three the experimental set up for studying the performance of the monocell probe of the cavity expansometer has been presented in detail. The observations and results using both unrestrained and confined expansion tests have been

presented in this chapter and discussed to highlight the probe performance.

In Chapter four the comparative study of the performance of the Cavitex in predicting the settlement, angle of shearing resistance ($\phi'$), pressuremeter modulus etc. have been presented.

General conclusions regarding the overall performance of the Cavitex have been presented in Chapter five. Scope of future studies has also been included in this chapter.

# 2 BRIEF DESCRIPTION OF CAVITY EXPANSOMETERS : A MONOCELL PRESSUREMETER

## 2.1 Brief description of cavity expansometer

In this chapter the basic features of the cavity expansometer and its operation have been presented.

*Control Unit :*

Except the design philosophy recently developed cavity expansometer is different from the models described in the literature. The equipment is hand operated and does not need any external source of pressure like a carbon dioxide cylinder. Figure 2.1 shows a schematic diagram of cavitex, showing the control unit and the probe. The various parts of the piston driving mechanism is shown in Fig. 2.2. for developing and releasing water pressure in cylinder. The piston can be driven in two modes, namely the rapid mode and the slow mode. In the rapid mode the Key is lifted up and the ram is rotated by means of a handle to achieve a rate of 6.35 mm/revolution. During the slow mode the key is inserted into a slot, made in the ram and the worm is rotated to advance the piston at a rate of about 0.1058 mm/ revolution. This corresponds to about 0.4801 cc/ revolution and 0.0145% radial strain/revolution or 0.0269% volumetric strain/revolution . The volume corresponding to a particular pressure can be obtained by multiplying counter reading with the least count (0.4801 cc/rev.).

The hydraulic circuit of the equipment has also been presented in Fig. 2.1. The cylinder outlet shown in Fig. 2.2 is

connected to an aluminium manifold through a copper tube. Four holes are provided in the manifold. The Bourdon type pressure gauges ($G_1$ and $G_2$) are connected to the holes. Inlet and outlet are provided through one port each. Four needle type valves ($V_1$ to $V_4$) are provided one at each port. The assembled circuit is shown in Fig. 2.1. The complete surface unit without external covering is shown in Fig. 2.2. The detailed description of the same has been given by Chauhan (1989).

*Monocell Probe :*

A brief description of the monocell probe is presented as follows:

A central pipe threaded at both ends passes through a pipe which is covered with a rubber membrane, folded inside at both the ends and pressed by two thrust caps. Rubber membrane is covered with 16 overlapping strips of stainless steel tucked by screws on the thrust caps. Longitudinal expansion of membrane is prevented by two semi flexible end-caps. An inlet copper tube is connected to the external pipe to inject water between the tube and rubber membrane.

The assembly is shown in Fig. 2.3. Some of the salient features of the probe are as follows :

1. Outside initial diameter 66mm (no expansion)
2. Maximum outside diameter 83 mm (corresponding to about 25% radial strain)
3. Total probe length 700 mm
4. Effective probe length 520 mm ($\frac{l}{d}$ ratio of 7.88)

5. Thickness of rubber membrane 2 mm

6. Type of rubber: natural.

## 2.2 Operation of Cavitex

*Deairing of Circuit :*

Even a small quantity of air in the circuit would result into volume losses. However, the presence of small quantity of air is taken into during the calibration process. The following steps are followed :

1. In lifted key position, valve $V_2$, $V_3$ and $V_4$ are closed. The water is poured through inlet funnel and piston is moved back by threaded arm.

2. Piston is moved in the forward direction rapidly so that air bubbles come out from surface unit. Again the water is poured through funnel and above procedure is repeated.

3. The piston is moved forward and backward several times keeping the valve $V_1$ and $V_2$ open alternatively.

When the circuit is deaired completely and the cylinder is fully filled up with water, the key is inserted so that the equipment can be operated in the slow mode. Flexible hydraulic hose-pipe is connected between the surface unit and the probe. Before connecting the hydraulic hose is deaired by siphoning.

# 3 PERFORMANCE STUDIES OF THE MONOCELL PROBE OF CAVITEX

## 3.1 General :

The volume measuring system, including the tubing, cylinder and probe are filled with clear water. The operation of filling and deairing of cavitex is carried out with great care. There is a possibility that air bubbles trapped in the system are so compressed under pressure that the air could go into solution, leading to volume changes that are not accounted for in the calibration. So proper deairing is very important.

In order to compute the true pressure deformation response of the soil, the pressure and volume losses which are inherent in the cavitex should be measured. The pressure actually applied by the probe to the bore hole wall is deduced from the recorded fluid pressure, where as the change in diameter of the cavity is related to the volumetric expansion of the probe and can be determined by proper calibration.

The method of calibrating the equipment in the laboratory has been discussed in this chapter. Laboratory experiments that have been performed in order to find the probe behaviour and to assess the accuracy of the calibration procedure have been described in the subsequent sections. Experiments have been conducted to study the probe deformation pattern. The test procedure and observations are presented in the following sections.

While finding the membrane reaction, the difference between unrestrained tests and confined inflation tests are emphasized. Global and local effects of end resistant on the

pressure distribution acting along the probe for representative level of pressure and deformation are also highlighted. A more reliable calibration procedure for membrane and overlapping steel strip reaction is described which is applicable to all types of rubber membranes.

## 3.2 Deformed shape of the probe during unrestrained expansion :

Direct observation during the free air expansion for pressure losses, shows that during unrestrained expansion test the deformed shape is as shown in Fig. 3.1(a). However, the probe can not deform as shown in the figure. In the free air expansion test most of the expansion takes place at centre of the probe but because of confinement such deformation is not possible under the actual field condition and the deformation could be as shown in Fig. 3.1(b). As such, to study the true behaviour it is necessary to test it under confined condition.

### 3.2.1 Experimental Set up and Testing Procedure :

For studying the probe deformation a cylindrical test tank 1.4m in height and 0.75m in diameter and made of G.I sheet was constructed. The dimensions of the tank was so chosen that the possibility of error due to end effects was not appreciable.

Five holes of 7mm diameter were drilled on the boundary of the tank along a vertical line at 10 cm intervals starting from a height of 37 cm from the bottom of the tank. Similar holes were drilled diametrically opposite to the previously drilled holes. The total distance between the top most and bottom most holes was

so chosen that it covered the effective length of the probe. The diameter of the holes were such that aluminium tubes of outer diameter 7mm and wall thickness 0.5 mm could pass easily through these . Through each tube a thick wire of 2mm diameter was placed. A circular metallic disc was welded at one end of each of the wires.

The probe and surface unit were deaired and connected together through connecting tube and passes through a guiding rod.

Sand was sieved through IS sieve so that sand particles greater than sand sizes were removed. To achieve a homogeneous sand bed, sand was poured in the tank by rain fall technique. The sieved sand was kept in a hopper whose position could be adjusted through pulley and rope arrangement. Sand was poured raising the hopper through a constant height of 5 cm. It was moved first along the circumference of the test tank and then bringing it toward the centre. This way sand had been placed upto a height of 25 cm and the probe was then placed in position at the centre of the tank with the help of a guiding rod. The probe was held vertically. Then the level of the sand was raised up to 37 cm. At this height two aluminium tubes as mentioned earlier were placed in position through the diametrically opposite holes as shown in the Fig. 3.2. The one end of each of the tubes was kept about 2 cm away from the probe and other end was projected out through the tank wall. To reduce the friction between the aluminium tube and the wire the tube was properly oiled using mobile oil. The wires were also dipped in mobile oil before inserting it through the aluminium tube. One end of the wire was placed in such a manner that it was in touch with the

probe surface and on the other end where the metallic circular disc was welded a dial gauge was mounted for measuring the probe deflection during the application of the fluid pressure. The sand was filled up to the full height of 1.4m.

The water from the cylinder of the control unit was injected in the slower mode through the connecting tube into the probe. As the water had been filled up into the probe it inflated and there by caused the wire to slides outward through the tube. This movement was measured by the dial gauge. The complete assembly is shown in Fig. 3.2.

The deformed shape of the probe has been shown in Fig. 3.3. It can be observed from the figure that the probe is distorted at the end zones but the central zone has cylindrical expansion pattern. It is also noted that the distorted zone at each end extends over a depth of 0.26 times the effective probe length where as the central zone extends over a depth of 0.48 times the effective probe length. The central zone is the zone which corresponds to the measuring cell of the Menard pressuremeter. A more precise determination of the zone could have been made by making displacement measurements near the ends of the probe at closer intervals. However, it may be concluded from the observed probe deformation that the choice of the $\frac{l}{d}$ ratio of 7.88 for the probe was correct. In Fig.3.4 the diameter at the centre of the probe and also the theoretical diameter corresponding to the different values of actual volume of the probe assuming uniform expansion of the probe has been presented. This gives an indication of the error due to the non uniform expansion, error has been observed to be about 1.3%.

## 3.3 Calibration Procedure, Observation and Inferences :

### 3.3.1 Volume Losses :

*Method I* : Various volume losses are inherent in the pressuremeter. These are due to expansion of the tubing which connects the control unit to the probe, compression of rubber membrane and metallic sheath, compression of water, presence of small quantity of air etc.

Calibration for volume losses was done by inserting the probe vertically into a close fitting, thick walled steel tube. The probe was inflated to seat against the sides of the tube. After that the probe cannot inflate any further and, as such, any volume change that was measured was due to the losses in the control unit. Because of the space between the probe and the steel tube, it takes certain volume and pressure to inflate the probe before it comes in contact with steel tube. A typical calibration curve is shown in Fig. 3.5. It is seen from the figure that at pressure 600 kPa there is good contact of the probe with the steel tube. At pressure greater than this, volume losses are in the control unit, the hydraulic cable and the probe. For pressure lower than this the straight line portion of the curve can be extended back to measure the volume losses. However, this method underestimates the correction. For low pressure range volume losses can be obtained by calibrating the control unit and the hydraulic cable without probe. The calibrating results are presented in Fig. 3.6. The composite correction curve has been drawn by using procedure suggested by Baguelin et al. (1978) and is presented in fig. 3.7.

*Method II* : The method described in the previous section to find the contact point may not give the exact value. So pressure volume curve was plotted in log-log scale as shown in Fig. 3.8. It can be seen from the figure that there is a sharp change in slope at pressure 50 kPa corresponding to volume 123 cc. So 123 cc of water is required to be injected into the probe in order to seat the probe against the sides of the tube.

Denoting by $L_a$ the active length of the probe and by $R_i$ the internal radius of the tube, the theoretical volume of the probe during the test can be computed by using the following relation

$$V_t = \pi R_i^2 L_a \qquad (3.1)$$

Subtraction of the volume of the fluid required to achieve full contact (123 cc) from the theoretical volume of the probe yields the initial volume of the tube. The correction of tubing expansion ($V_c$) is expressed as

$$V_c = V_n - V_t \qquad (3.2)$$

where $V_n$ is the nominal volume of the probe which is obtained by adding the volume of fluid injected ($V_j$) to the initial volume ($V_i$). The typical curve of Fig. 3.7 shows the volume losses at different pressure. The Method II presents better estimation of the volume losses for higher pressure.

### 3.3.2 Pressure Loss

#### 3.3.2.1 Standard Calibration Procedure

As the probe inflates certain amount of pressure is necessary to overcome the resistance of the rubber membrane and the steel seath. Thus the pressure which is actually applied to the soil is less than the fluid pressure in the probe.

While calibrating for the pressure loss the probe was placed upright simulating the vertical placement of the probe in the field. The pressure calibration was then done by expanding the probe in the air and measuring the pressure at different volumes. Calibration was done at the same strain rate as used during field testing. The obtained pressure correction curve due to membrane resistance in the cavitex is superimposed on similar curves for Menard pressuremeter in Fig. 3.9 [after Baguelin et al. (1978)]. It can be seen that the membrane correction for cavitex is smaller compared to other pressuremeters. The procedure was first adopted by Chauhan (1989) in calibrating the cavitex. The same has been adopted in recalibrating the equipment as it was not used for more than 2 years. It can be seen from the figure 3.9 that there is a marginal difference between the curve obtained by Chauhan (1989) and the present curve. This may be due to fact that the rubber membrane used in the present study is different than the one used by Chauhan (1989) though both were made in the same lot.

### 3.3.2.2 Improved Calibration Procedure :

*Theory* : The improved calibration technique as suggested by Murat and Lemoigne (1988) was also adopted in the present study.

Assuming a plane stress condition, a relation between internal pressure ($p_i$) in a ring and circumferential strain ($\epsilon_\theta$) can be given by

$$p_i = \frac{E}{2}\left(\frac{R_e^2}{R_i^2} - 1\right)\epsilon_\theta \qquad (3.3)$$

where E is the modulus of elasticity of the ring. The subscript 'e' and 'i' denoted the external and internal respectively.

*Experimental Procedure :*

In order to perform a detailed analysis of the membrane behaviour under representative level of pressure and deformation, a series of tests was performed by confining the probe inside an instrumented aluminium tube. The internal and external diameter of the tube were 75 mm and 81 mm respectively. The tube consisted of a stack of five rings of identical diameter and of different length, held loosely together by two end plates. On each ring two strain gauges of the following specification

| | | |
|---|---|---|
| Manufacturer | : | Transens |
| Type | : | SA-12-3T |
| Gauge Factor | : | 2.15 |
| Resistance | : | 121Ω |

were mounted on the outer surface of the ring diametrically opposite to each other at the mid height of the ring. The strain

gauges were mounted on the surface as follows.

The ring surface at appropriate places were cleaned by rubbing it by emery paper (No-400).Then the rubbed surface was cleaned with acetone. Finally the glue was spread over the cleaned surface and soon after that strain gauge was kept over this glue. A piece of polythene sheet was then placed over the strain gauge and pressed gently by thumb in such a manner so that no air entrapment took place. After this adhesive tapes were placed over the strain gauge and it was left over for 24 hours for drying. Each strain gauge was soldered to thin plastic coated aluminium electrical wire. The position of strain gauges are shown in Fig. 3.10.

The probe was inserted into the stack of rings which had been previously marked as 1,2, ...,5. The connecting wires were connected to the strain gauge indicator (Model P. 350 AZ, 115 V 250 S/N 45905, Instrument Division, Measurement group, North Carolina, USA.). The strain gauge indicator setting was made to correspond to the gauge factor 2.15 of the used strain gauges. The quarter bridge circuit was used for measurement. The strain gauge indicator was then adjusted to find the null point. Fine adjustments were then made to increase the sensitivity of the measurements and again the strain indicator was adjusted for finding the null point. The reading corresponding to this setting is treated as the initial reading.

Pressure was then introduced in the rings through the hydraulic cylinder of the control unit operating it in the slow mode. As the pressure developed in the ring the null setting was disturbed. The strain indicator was again adjusted for null set.

The final reading corresponding to this setting was noted down. The difference of the final and the initial readings indicated the level of strain in the ring due to the applied pressure. The average strain levels indicated for the opposite strain gauges was taken as the strain in the ring. The complete assembly is shown in Fig. 3.11

To find the modulus of elasticity E of the aluminium a specimen was prepared from the tube and tested using Instron 1195 universal testing machine. The modulus of elasticity `E' was computed from the linear range of the curve. The computed value of E is 66.66 GPa.

*Pressure distribution along the probe length :*

In order to obtain the pressure distribution along the probe length fluid pressure was supplied in incremental stages. The corresponding readings in strain in the ring were obtained by strain indicator. The pressure actually transferred to the rings was then computed from the measured strain values using the stress strain relationships as shown in equation 3.3. The typical result showing the relationship between the applied fluid pressure and the pressure developed in the ring sets is illustrated in Fig. 3.12. The abscissa represents the distance from the bottom of the probe and ordinate represents fluid pressure. From the Fig. 3.12 it is evident that only in the central portion of the probe more or less uniform fluid pressure is exerted to the tube. The pressure drops sharply and continuously near the end of the probe. However, the average pressure transmitted over the central portion was observed to be less than the applied fluid pressure.

This is due to the resistance in the membrane and the covering overlapping steel strips.

Fig. 3.13 (a,b,c) shows the variation of the internal pressure with time for various applied fluid pressure. It can be seen that in the rings corresponding to numbers 2,3 and 4 the internal pressure values do not differ appreciably where as in the ring 1 and 5 the discrepancy is large due to end effects. It is also seen from these figures that there was no significant loss of pressure with time and the pressure time variation may be considered to be more or less uniform over the period of testing.

*Pressure Loss Calculation :*

It was realised from the review of literature that experiment with a set of rings would be more cumbersome than the experiment conducted on single instrumented tube of same size.So before cutting the tube, the same experiment as described in previous section was conducted on a single instrumented tube. The internal pressure of the single instrumented tube as computed from strain measurements in the tube compare reasonably well with the average pressure as previously obtained for the instrumented ring stacks. The pressure difference between the two observation is pressure loss.

The probe was kept inside the tube having the same length as that of the probe. Strain gauges were fixed as described earlier at mid height of the tube. The probe was inflated increasing the fluid pressure in stages. For each pressure increments the circumferential strain as well as the amount of fluid supplied to the probe were noted.

The internal pressure in the tube was computed from the stress-strain relationship as described earlier. The variation of the applied fluid pressure, the developed internal pressure and the pressure loss with time is shown in Fig. 3.14. The studies made with single instrumented tube and single instrumented stack of rings show that the pressure loss in the probe in the two cases are as given in the Table 3.1.

Table 3.1
The comparison of pressure loss between improved and standard calibration procedure

| Volume (cc) | Membrane and steel strips resistance by Imp. Calib. kPa (Using Single tube) | Membrane and steel strip Resistance by std.calib.(kPa) | % difference |
|---|---|---|---|
| 480 | 17 | 35 | 53% |
| 487 | 12 | 35.75 | 65.5% |
| 495 | 15 | 35.50 | 57.74% |
| 498 | 21 | 35.75 | 41.54% |
| 502 | 30 | 36.00 | 16.80% |
| 504.5 | 24 | 36.29 | 33.80 |
| 506 | 24 | 36.50 | 34.84 |
| | | Average | 43.28 |

The table reveals that the previous procedure of probe calibration (Baguelin et al. 1978) is much inferior to the improved calibration procedure (Murat and Lemoigne, 1988). The use of the first technique may lead to substantial error (43.28%) in

predicting the pressure loss due to probe resistance. The observed pressure loss by using both the techniques as described is also presented graphically in Fig. 3.15. The figure clearly brings out the qualitative difference of the two probe calibration procedures.

# 4 PERFORMANCE OF CAVITEX IN SAND

## 4.1 General :

Performance of the Cavitex in local silt deposits of I I T Kanpur campus was studied by Chauhan (1989). In this chapter its performance in sand has been presented. Cavity expansometer test results were analysed to predict strength parameters, bearing capacity and settlement of foundation. These were further cross examined by either laboratory or field tests to check the reliability of the predictions.

## 4.2 The Site :

The I I T Kanpur campus is located on the thick alluvial deposits of river Ganga. The soil deposit contains silt with little amount of clay and sand. The ground water table changes considerably with the change of seasons. A test sand bed was prepared in this soil deposit to study the performance of the cavity expansometer. The site was dug upto a depth of 2.75 m and the soil was replaced by Ganga sand to prepare the test bed. Below this depth lie the local soil deposits. No special effort was made to get a homogeneous bed. The bed was previously made by the staff members of Geotechnical Engineering Laboratory.

The field tests were performed in November 1990 and no water table was observed upto a depth of 4.5 m. Fig. 4.1 shows the field test locations at the experiment site.

## 4.3 Test Conducted :

The following tests were conducted at the site

i) Standard Penetration Test (SPT)

ii) Static Cone Penetration Test (SCPT)

iii) Plate Load Test (PLT)

iv) Strain controlled Cavity Expansometer Test (Pressuremeter Test, PMT)

As the SPT, SCPT and PLT are standard field tests, the procedures for doing the tests are not described here. Only the strain controlled pressuremeter test using cavity expansometer is briefly described.

### 4.3.1 Strain Controlled Cavity Expansometer Test

Tests were conducted in a prebored hole. Soil disturbance due to stress relief in a prebored hole, especially in loose cohesionless soil is usually significant. Since result of the pressuremeter tests are highly sensitive to the soil disturbance, a standardized procedure is used to make the hole and conduct the test. Best quality of bore hole is obtained with hand augering (Baguelin et al. 1978). To make the bore hole with minimum disturbance, two stage augering was done. First, bore hole of 60 mm size was augered with the helical auger and finally the bore hole was enlarged to 68 mm size with another helical auger.

The probe was then lowered into the bore hole with the help of a guiding rod upto the desired depth of testing. The probe was then inflated by injecting water at a constant rate of approximately 2% volumetric strain per minute. The volume readings were taken at every 20KPa pressure interval. Tests were conducted at 0.5 m, 1.5 m and 2.0 m depths. During the tests the equipment

performance was satisfactory; there were no problem of leakage, memberane coming out from the grip, membrane puncture or bursting.

## 4.4 Results, Discussions and Inferences :

Fig. 4.2 shows the grain size analysis with depth. Fig. 4.3 shows the strata variation along with the SPT blow count and natural water content. The soil has been classified as per I.S. 1498-1970. It can be seen that soil upto 2.75m depth is poorly graded sand and below it is predominantly silt with presence of clay and sand. Fig. 4.3 shows the variation of both uncorrected and corrected N values and soil classification with depth. For overburden correction Peck et al., (1974), equation was used in the analysis. Variation of cone resistance with depth is shown in Fig. 4.4.

Load settlement diagram obtained from Plate load test on circular plate is shown in Fig. 4.5. The same result is replotted on log-log graph sheet in Fig. 4.6 which clearly shows the load corresponding to local shear whereas in the Fig. 4.5 the same is not very obvious. After applying the corrections the pressuremeter test results are plotted on natural as well as on log scale as shown in Fig. 4.7 and 4.8(a,b,c) respectively. Following parameters are obtained from pressuremeter test :

Value of $P_o$ is estimated from the initial portion of the curve where the Kink of the line was observed. Limit pressure ($p_l$) and the pressuremeter modulus were also estimated using the approach as described in sections 1.3.4 and 1.3.5 of the introduction. Fig. 4.9 demonstrates that $p_o$, $p_l$ and $E_M$ bears a

linear relationship with depth. Similar relationships were obtained for the loose sand deposits and for very stiff marl (Baguelin,1978).

$K_o$ value for the sand deposits were obtained from the test results at depth 0.5, 1.5 and 2.0 m respectively. The average value of $K_o$ is 0.589. The same computed using Jaky's relationship is 0.44. The difference between the two values was observed to be 25%. In estimating the value of $K_o$ using the Jaky's relation the value of $\phi'$ as obtained by direct shear test was used. When the value of $\phi'$ obtained from PMT was used the value of $K_o$ was 0.478, which was very close to the value of 0.44. The percentage difference between these values was only 8.6. The unit weight of sand required to compute the $K_o$ values from the $p_o$ values was determined as 16.5 $KN/m^3$ by sand replacement technique. The bearing capacity of a 30 cm circular plate was estimated by using the value of $\phi'$ predicted from PMT. Using Terzaghi's bearing capacity equation. The estimated value were 230 $Kn/m^2$ and 78.37 $Kn/m^2$ at 0.5 m depth for general and local shear failure conditions. The value obtained from plate load test was 240 $KN/m^2$.

The bearing capacity was also estimated directly by using the co-relation proposed by Baguelin et al. (1978). However, the predictions were very much off from the observed value from the plate load test. As such, these results are not presented here in. The probable reason for the discrepancy is that the factor proposed by Baguelin is not valid for Ganga sand. So the value of k was estimated by using the Terzaghi's bearing capacity equation and the estimated $p_l$ and $p_o$ from the cavity

expansometer test, for both local and general shear failure conditions. The values of k has been superimposed on the curves Fig. 4.10 suggested by Beguelin et al. (1978). It may be observed that for the general shear failure case the curve for $p_l$ equalto 300 kPa the predicted curve for the present study agrees well with the corresponding curves suggested by them. However, the curve corresponding to local shear failure case is quite far off from the corresponding curve.

Settlement of 30cm circular plate was estimated from CPT test data using Schmertmann's method, pressuremeter test result and compared with actual value as obtained from plate load test.

From Fig. 4.6 the settlement of the 30 cm circular plate corresponding to the pressure of 240 $KN/m^2$ causing local shear failure was obtained as 11 mm. The same as estimated from CPT data by using Schmertmanns method was 10.56 mm. The corresponding figure from the cavity expansometer data was 13.5 mm. The detailed computations of the settlement as estimated is presented in Appendix I. In Table 4.1 the errors in prediction for the different predictive models with respect to the observed values have been presented

Table 4.1

Comparision of settlements obtained by different methods

| Method | CPT | Cavitex | PLT |
|---|---|---|---|
| Settlement(mm) | 10.56 | 13.46 | 11 |
| % error | -4 | 22 | 0 |

It can be seen from the table that the best prediction is achieved from CPT results, However, the prediction achieved from cavity expansometer test results was also in good agreement with the observed value and the error is within the tolerable limits and is on the safe side.

Static cone penetation test result can be used to determine approximate value of $\phi'$ for the sand. The resulting value of $\phi'$ are compared with those obtained from the cavity expansometer tests as shown in Table 4.2. Predictions for the CPT results were made using the suggestions made by Meyerhof (1976) whereas the same for cavitex were made by using Gibson and Anderson theory (1961)

TABLE 4.2

Comparison of the angle of shearing resistance obtained by different methods

| Depth | $\phi'$ | | | |
|---|---|---|---|---|
| | CPT | PMT | PLT | DST |
| 0.5m | $30^{o}30'$ | $31^{o}30'$ | $35^{o}$ | $34^{o}$ |
| 1.5m | $33^{o}25'$ | $32^{o}30$ | | |
| 2.0m | $30^{o}40'$ | $31^{o}30'$ | | |

The table 4.2 shows that the predictions made for CPT and PMT observations are on the lower side than that obtained for PLT and Direct shear test (DST) results.

The condition of soil can be determined from the pressuremeter test results. Table 4.3 provides such information (Baguelin, 1978)

TABLE 4.3

Strata, state description from PMT and SPT Observations

| $p_l$ (KPa) | Description | SPT (N) |
|---|---|---|
| 0 - 200 | very loose | 0 - 4 |
| 200 - 500 | loose | 4 - 10 |
| 500 - 1500 | compact | 10 - 30 |
| 1500 - 2000 | dense | 30 - 50 |
| $2500^+$ | very dense | $50^+$ |

It can be seen from Fig. 4.3 that upto a depth of 2.75m the SPT N lies between 4 to 10 signifying the deposit to be in the loose state. The cavity expansometer test shows that the limit pressure lies in the range of 200-500 KPa. This also signifies a loose state of sand. So it can be inferred that prediction regarding the state of sand grains packing from the cavity expansometer test is also very reliable.

In Fig. 4.11 data from the present investigations has been superimposed on the results obtained by some investigators (Baguelin et al. 1978). Though a large scatter was observed as shown in the graph by Baguelin (1978) be adopted for sands, and for sand Baguelin (1978) recommend $\frac{N}{p_l} = 2 \times 10^{-2}$. In the present investigation the average value of $\frac{N}{p_l}$ of the three test results has also been found to be $2 \times 10^{-2}$ for the Ganga sand.

. The ratio $\frac{q_c}{p_l}$ varies from one site to another. Dilatancyis an important factor for sand. The ratio of $\frac{q_c}{p_l}$ provides a reliable indicator to find the possibility of influence of the dilatancy. If the ratio is of the order of 5 to 6, soil is non-dilatant and if its value is 8 , 10 or 12 it is dilatant.

In Fig. 4.12 ratio of $\frac{q_c}{p_l}$ as a function of $q_c$ as obtained from the present test is superimposed on the results presented by Baguelin et al. (1978). It can be seen from the figure that the data for Ganga sand obtained from the present investigation compares very well with those obtained for Hydraulic sand fill. It can be seen that there is a small increase in the $q_c/p_l$ ratio with increasing $q_c$. $q_c$ is influenced to a greater degree than $p_l$ by the analysing the state of soil. In present study $\frac{q_c}{p_l}$ is found to be 6.78, 6.66, 4.41 corresponding to the 0.5, 1.5 and 2.0 m depth. So the soil is non-dilatent type which confirms to the previous finding that the sand deposit is in a loose state.

# 5 CONCLUSIONS AND SCOPE OF FUTURE WORK

## 5.1 Conclusions :

Following conclusions are drawn on the basis of the present work.

1.(a) Expanded shape of the central potion of the probe within the soil is cylindrical and extends over about 48% of the effective length of the probe signifying that the designed L/d ratio of the probe is very good. On either side of this portion the probe deformation is non-uniform.

(b) Pressure distribution around the probe in the central portion is more or less uniform.

(c) Improved calibration procedure using restrained expansion of the probe gives pressure loss about 45% less than that obtained from free air expansion calibration procedure.

(d) In unrestrained expansion there is a ballooning effect during expansion of the probe thereby excluding a full inflation. Furthermore, the resulting deformed shape varies greatly from that obtained under actual testing conditions. So, improved calibration is more reliable because expansion is cylindrical over a considerable portion of the probe

2. The result obtained from the present study using cavitex with monocell probe in loose sand deposits compares reasonably well with those reported in the literature for similar deposits obtained by using tricell

pressuremeter testing equipments.

3. Predictions made by cavitex test observations are in good agreement with those obtained from other test like static cone penetration test and plate load test.

4. Performance of the equipment in the field was entirly satisfactory. No leakage was observed in the hydraulic circuit during the test.

## 5.2 Scope of Future Work :

1 Present improved calibration is done for intermediate deformed shape of the probe. So the calibration for initial and maximum deformation of the probe should be conducted to study the probe behaviour over the entire range.

2 The probe behaviour studies can be done for different temperatures.

3. Detailed comparisons of pressure volume curve between cavity expansometer test and other conventional pressuremeter tests need to be carried out.

4 Following Modifications are possible in the Cavitex :

a Probe membrane suitable for high pressure can be developed by properly reinforcing the membrane in the longitudinal directions.

b Single vent hole in the cylinder of control unit causes difficulties in deairing. To remove the difficulties additional vent hole at the top surface of the end of the cylinder can be made.

c In deep bore holes greater than 10m, expansion of the probe due to hydrostatic head will cause suction in the cylinder. To overcome this problem, resistance of the rubber membrane should be increased in lateral directions.

d Introduction of electric prime mover with a gear system to automate the driving mechanism for removing the difficulties associated with manual driving.

## REFERENCE


1. Baguelin, F., Jezequel, J.F. and Shields, D.H (1978), The Pressuremeter and Foundation Engineering, Vol. No.4 in Trans Tech Publication Series on Rock and Soil Mechanics. First Edition 1978.
2. Chauhan, S.P. and Basudhar, P.K. (1990), Development of Low Cost Monocell Pressuremeter, Proceedings of the First International Seminar on Soil Mechanics and Foundation Engineering of Iran, Vol. 2, pp. 107-121.
3. Chauhan, S.(1989) "Development of a strain Controlled Pressuremeter", M.Tech. Thesis, I I T Kanpur, India.
4. Craig, R.F. Soil Mechanics (1983), English Language Book Society/Van Nostrand Reinhald (U.K.)
5. Hughes, J.M.O., Wroth, C.P. and Winole, D., (1977) Pressuremeter Tests in Sands Geotechnique 27 (4), 455-477.
6. Lambe, T. and Whitman, R.V. (1969), Soil Mechanics, S.I. Version, John Wiley and Sons, New York.
7. Mair R.J. and Wood, D.M. (1987), Pressuremeter Testing Methods and Interpretation, CIRIA Ground Engineering Report In-situ Testing.
8. Murat, J.R and Lemorgne, Y(1988)"Improved Calibration and Correction Techniques for Pressurementer," Geotechnical Testing Journal GTJODJ, Vol. 1, No.3 Sept 1988, pp 195-203.
9. Gibson, R.E. and Anderson, W.F., ( 1961), In-situ Measurements of Soil Properties with the Pressuremeter, Civil Engg. Public Wks. Rev. 56 ( 658 ), 615-618.

# APPENDIX

## SCHMERTMANN'S SETTLEMENT ANALYSIS

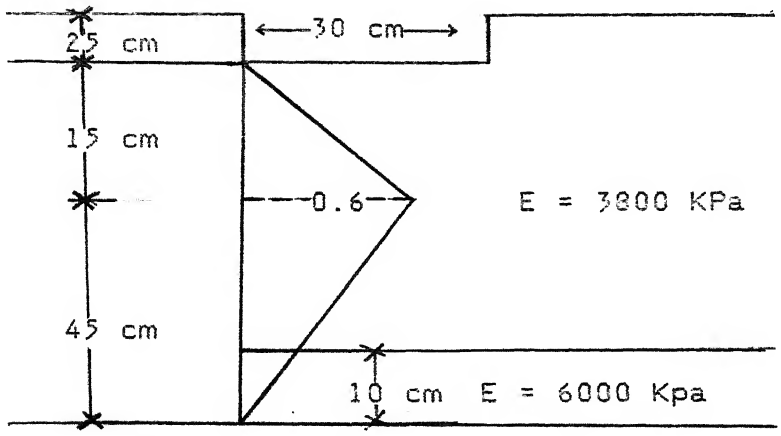


| Layer | Δz(m) | $E_z$(Mpa) | $I_z$ | $\frac{I_z \Delta z}{E_z}$ |
|---|---|---|---|---|
| 1 | 0.50 | 3.8 | 0.333 | 0.0438 |
| 2 | 0.10 | 6.0 | 0.067 | 0.001166 |

$\Sigma$ 0.0449

$$C_1 = 1 - 0.5 \frac{\sigma_o'}{q_{net}}$$

$$C_1 = 1 - 0.5 \frac{0.25 \times 16.5}{240}$$

$$= 0.98$$

$$C_2 = 1 + 0.2 \log e \frac{t}{0.1} \simeq 1$$

$$s = C_1 C_2 \left(\frac{I_z \Delta_z}{E_z}\right)$$

$$= 0.98 \times 1 \times 0.0449 \times 240$$

$$= 10.56 \text{ mm}$$

Pressuremeter test analysis :

From the plot of settlement coefficient verses width of footing (Fig. 1.1), one can obtain for the plate of 30 cm diameter, on sand.

$$f = 17$$

$$s = \frac{q_{net}}{E_m} f$$

$$= \frac{240}{3033} \times 17 = 13.46 \text{ mm}$$

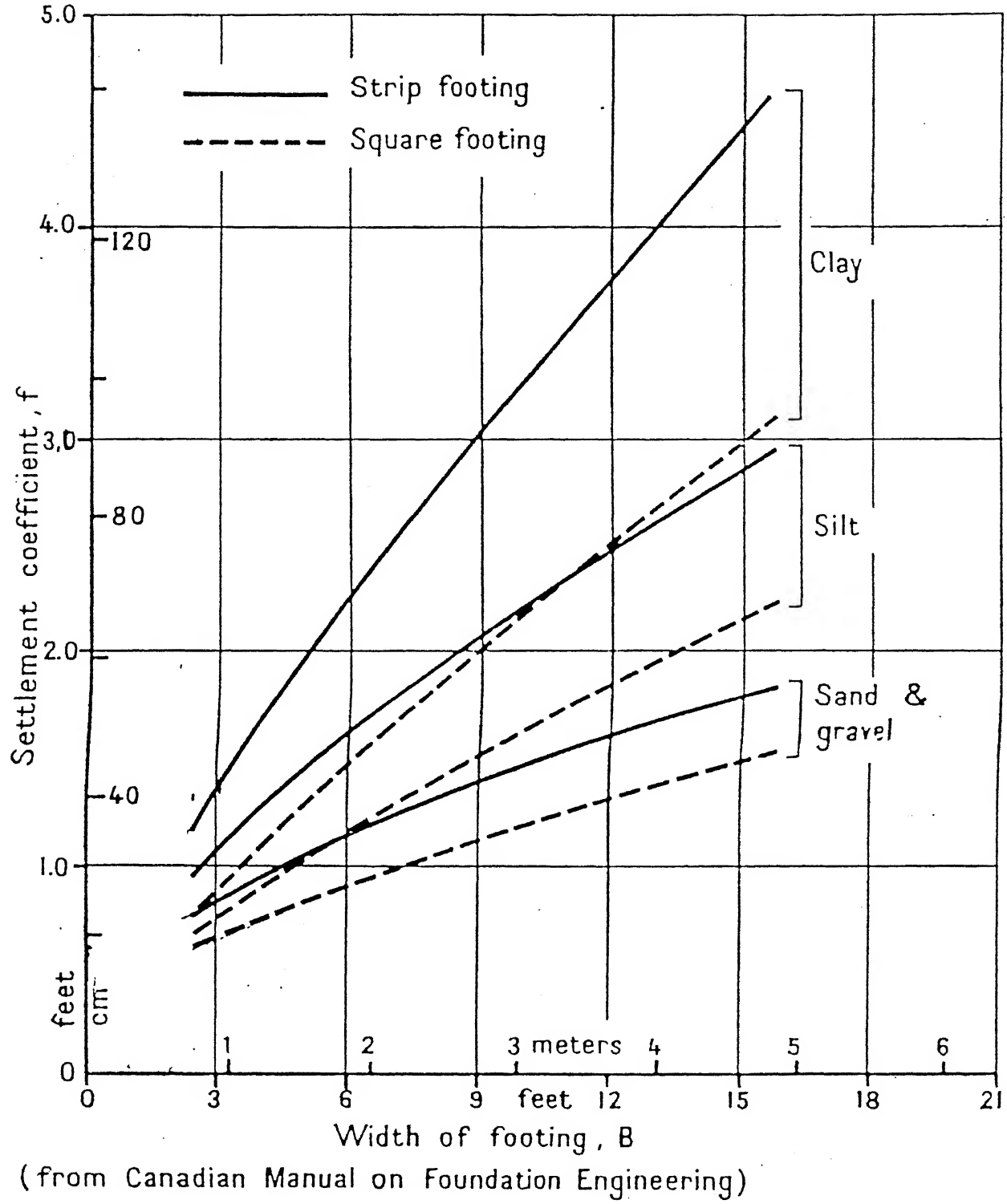


Fig. 11 MÉNARD's settlement coefficients.

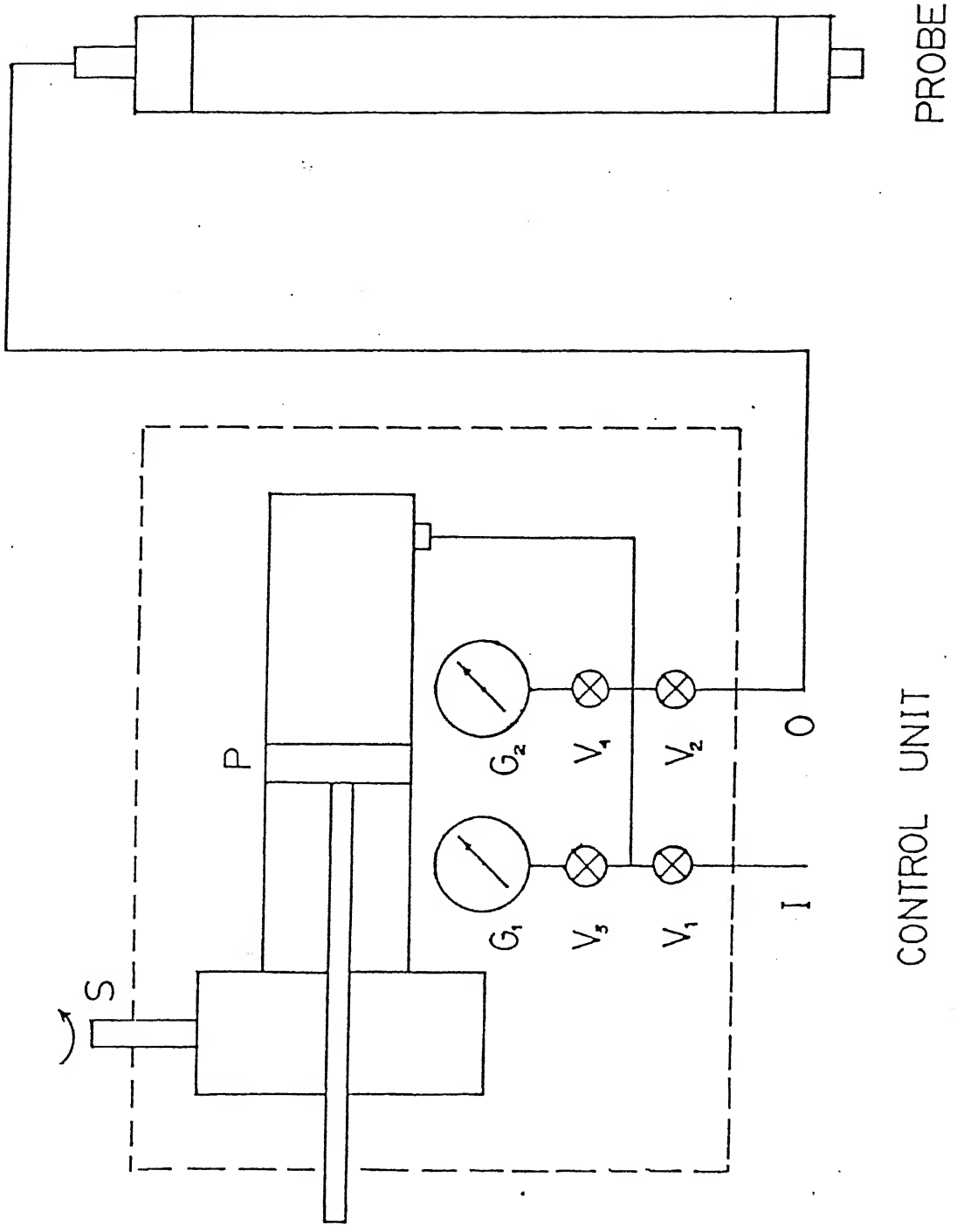


FIG. 2.1 SCHEMATIC DIAGRAM OF CAVITEX

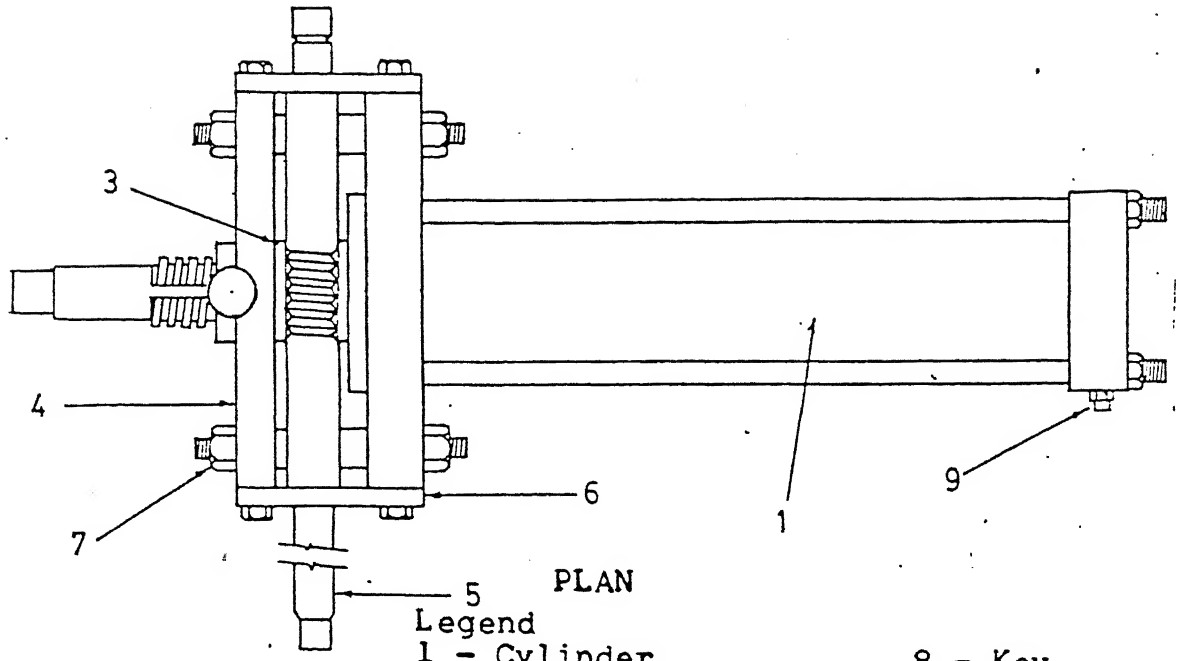


PLAN

Legend

1 - Cylinder
2 - Ram
3 - Threaded Worm Wheel
4 - Front Plate
5 - Handle
6 - Side Plate
7 - Four Studs
8 - Key
9 - Cylinder Outlet

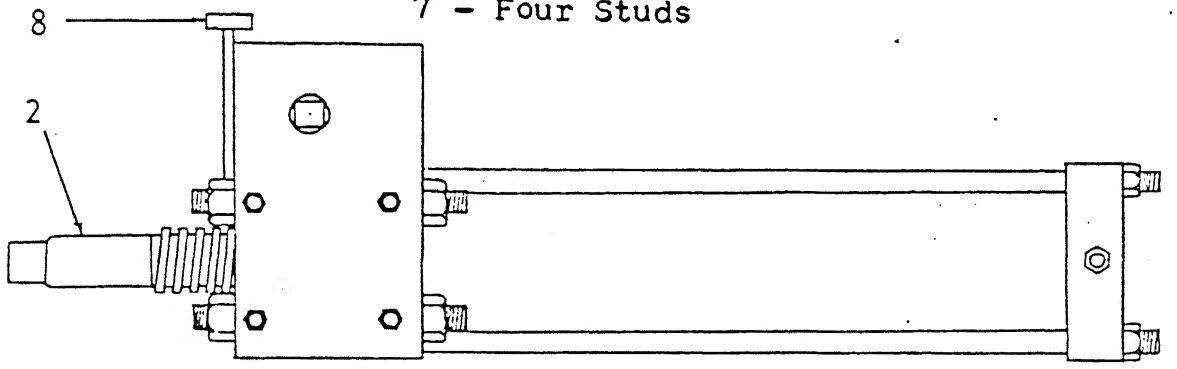


ELEVATION

FIG. 2.2 PISTON DRIVING MECHANISM

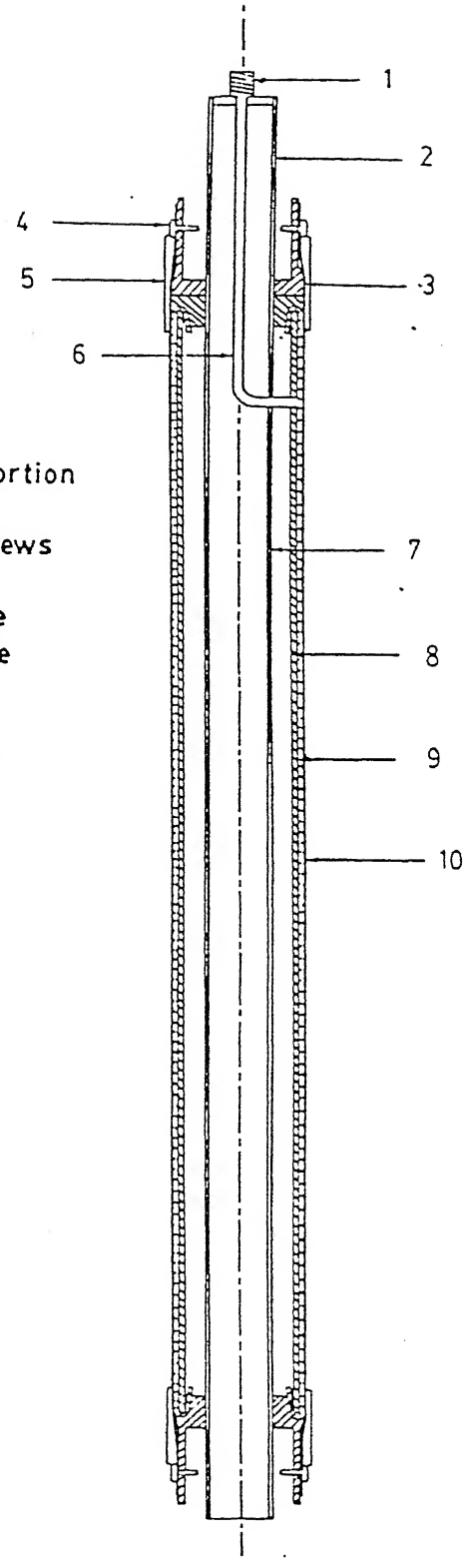


LEGEND

1. INLET
2. Threaded portion
3. Thrust cap
4. Tucking screws
5. End cap
6. Copper pipe
7. Central pipe
8. Outer pipe
9. Membrane
10. Steeljacket

FIG. 2.3 THE MONOCELL PROBE

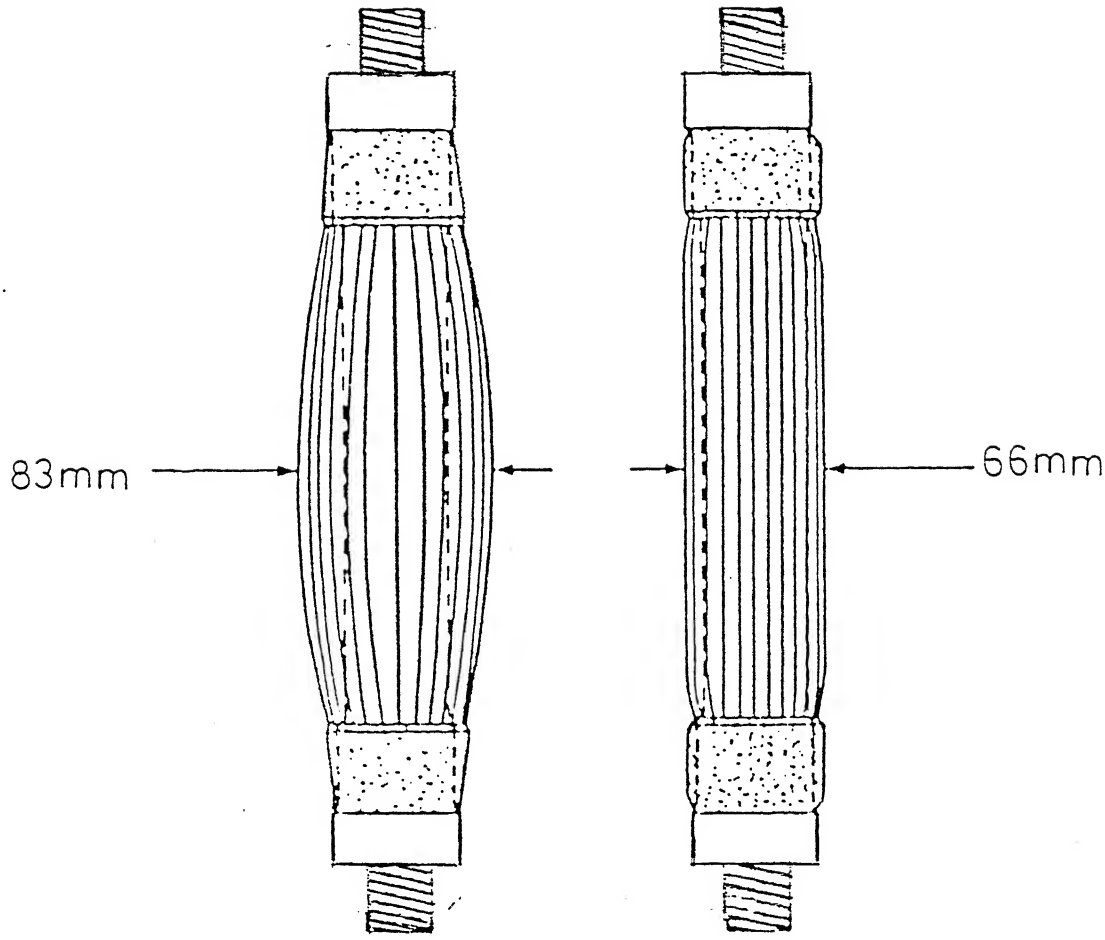


FIG 3.1 – *Deformed shape of the probe during* (a) *unrestrained expansion and* (b) *confined expansion (both of them for the same injected fluid volume).*

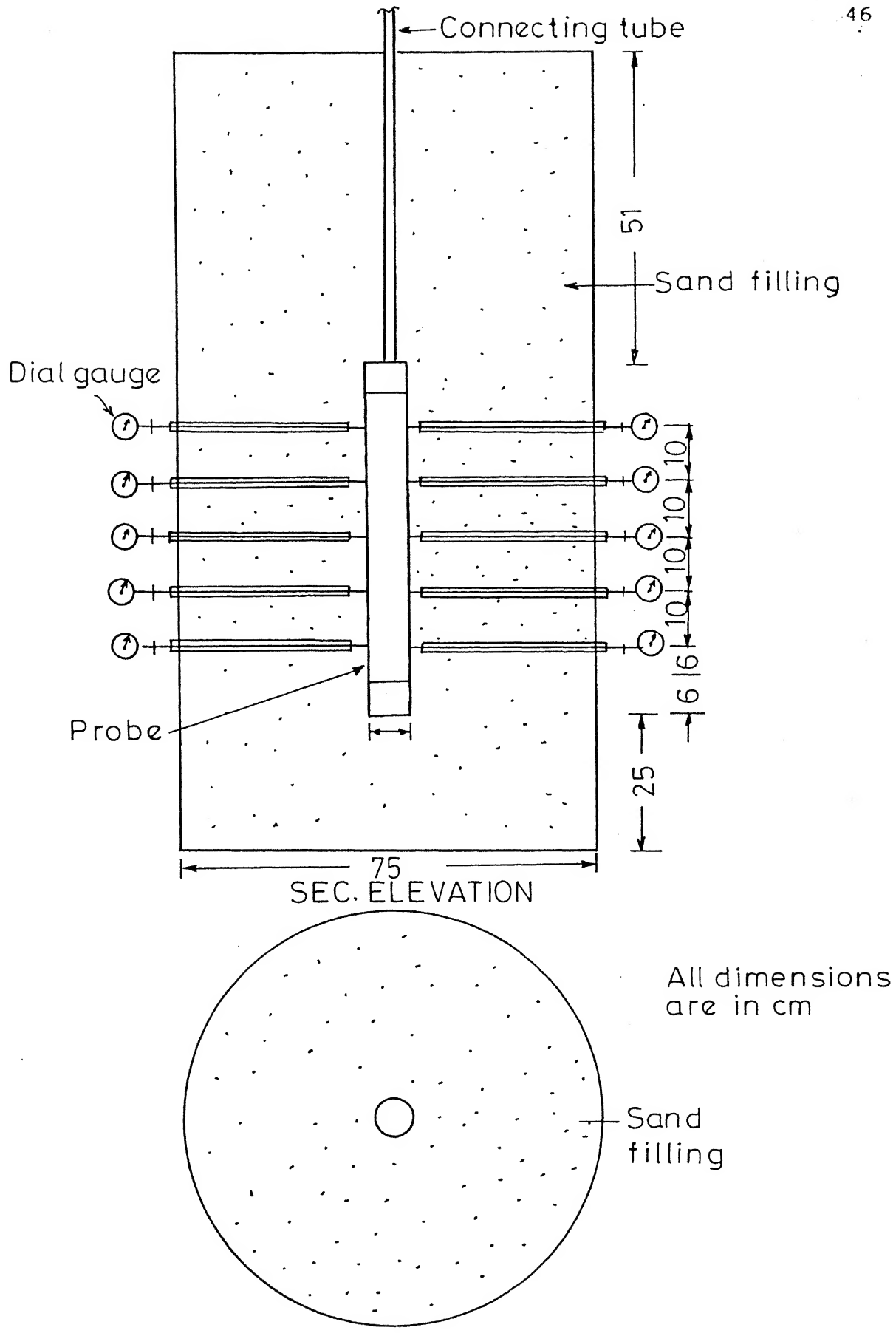


FIG. 3·2 EXPERIMENTAL SET-UP FOR FINDING PROBE DEFORMATION

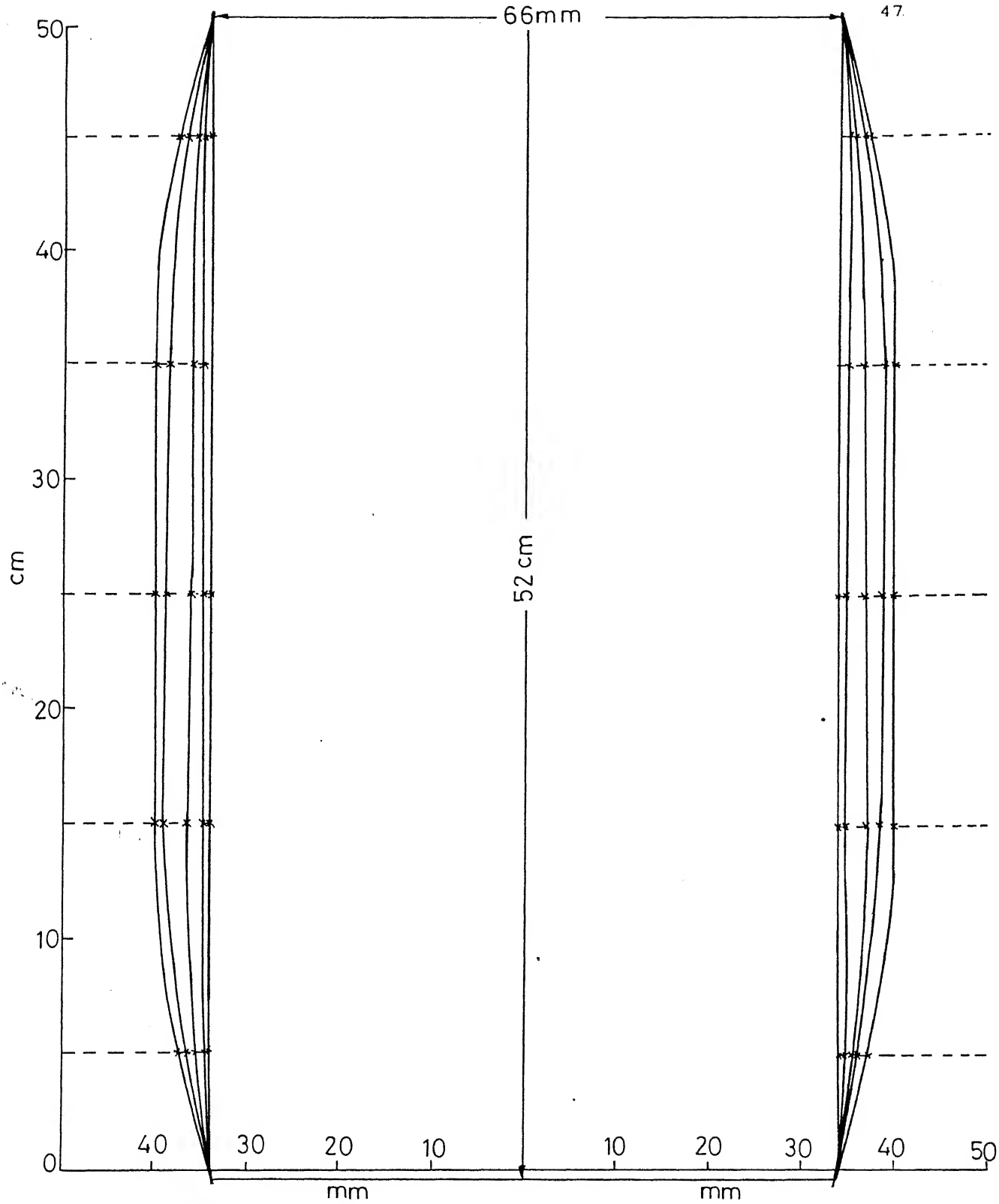


Fig. 3·3 Deformed shape of probe during confined expansion

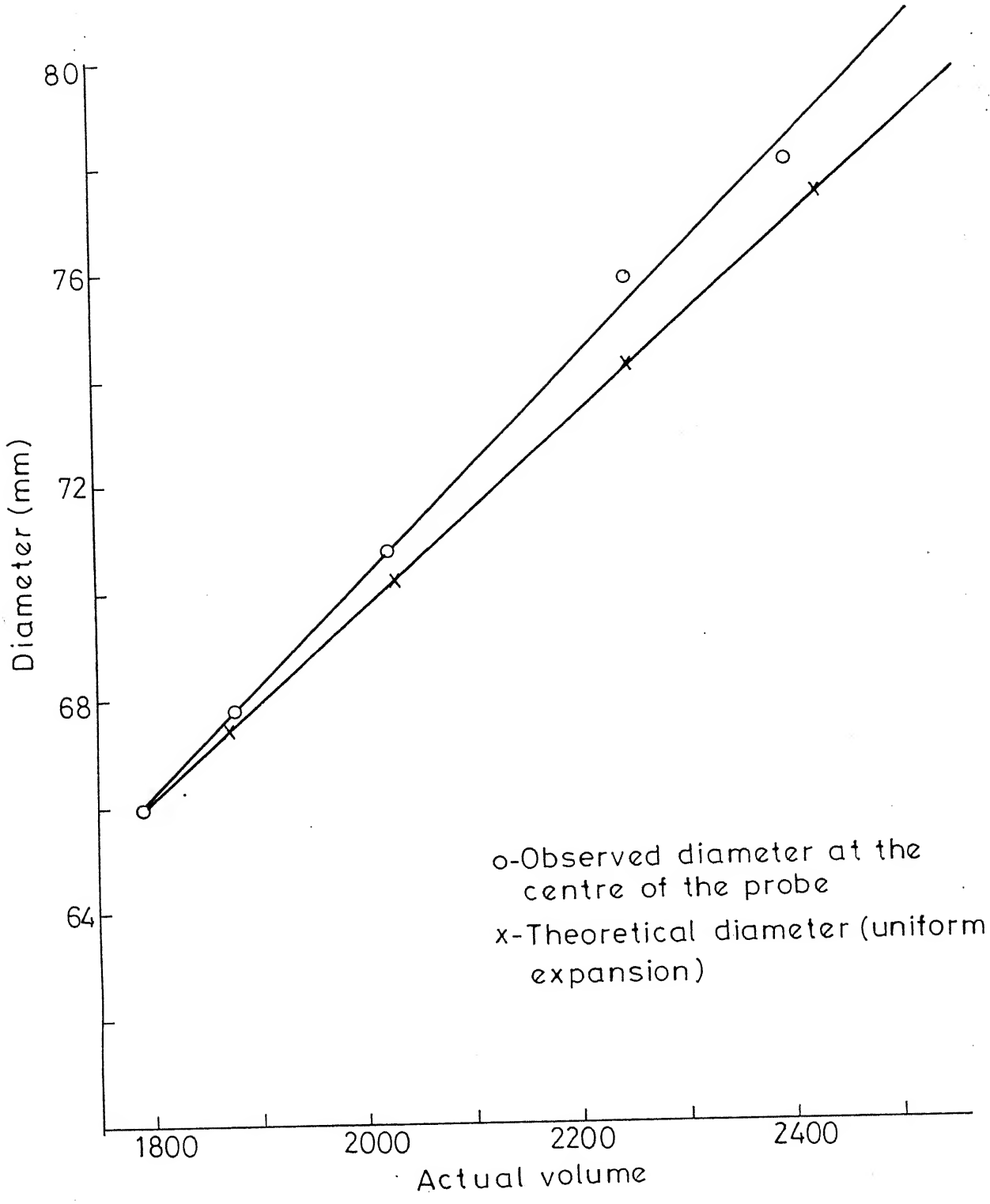


Fig 3·4 Comparison of the theoretical and observed diameter of the probe under field test condition

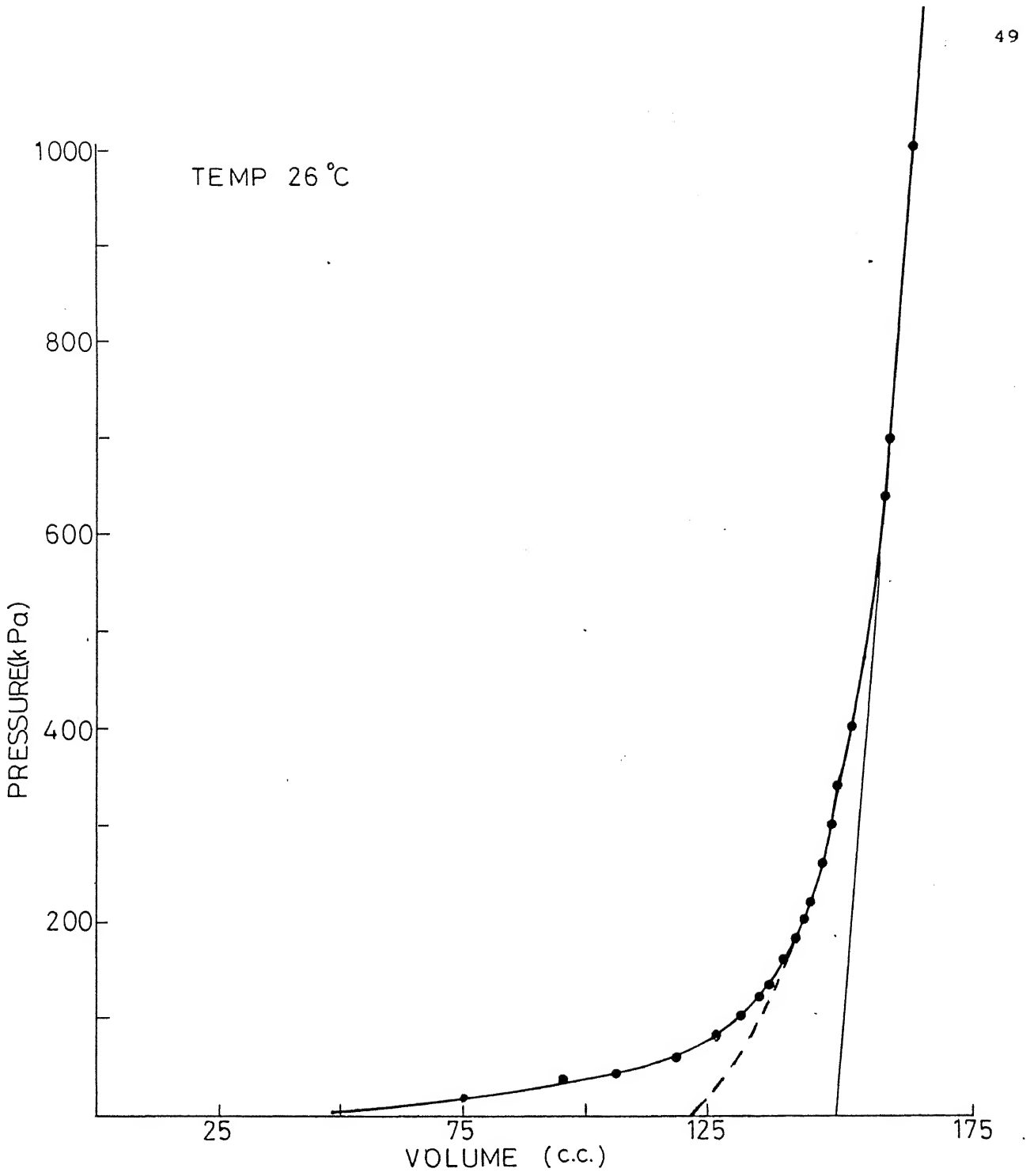


Fig. 3·5 Volume calibration curve (probe inside the tube

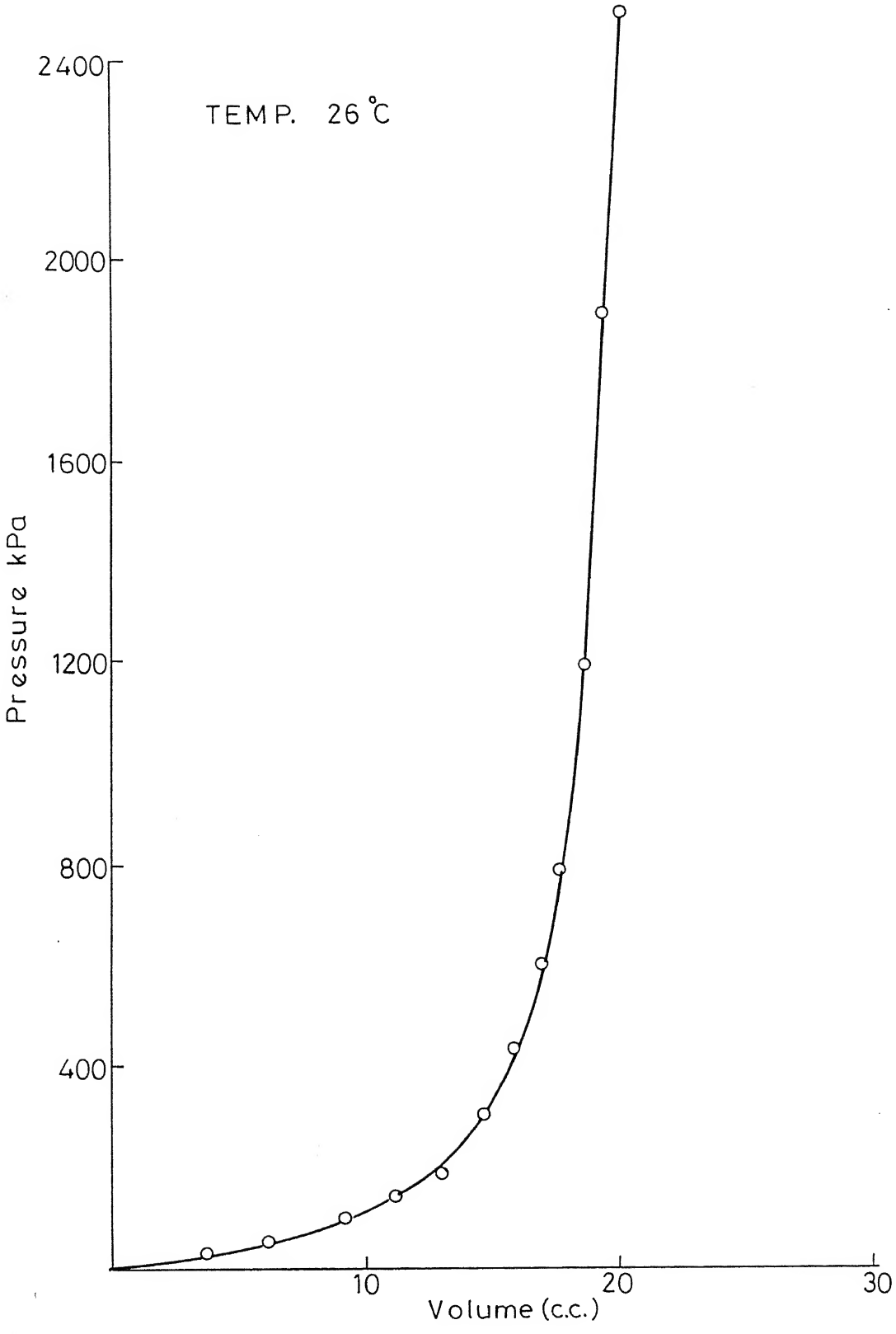


Fig.3·6 Volume calibration without probe

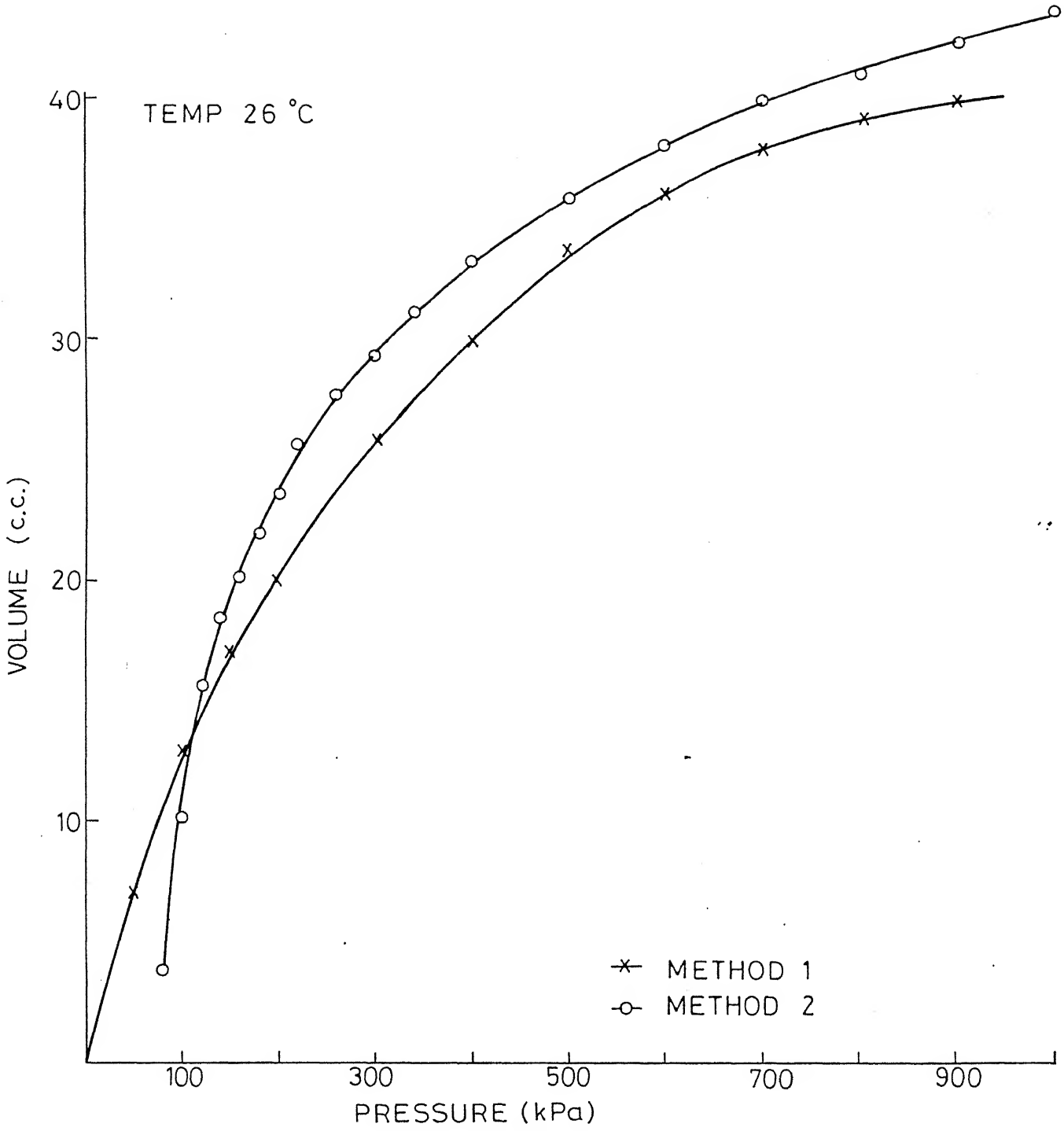


Fig. 3·7 Volume loss pressure relationship

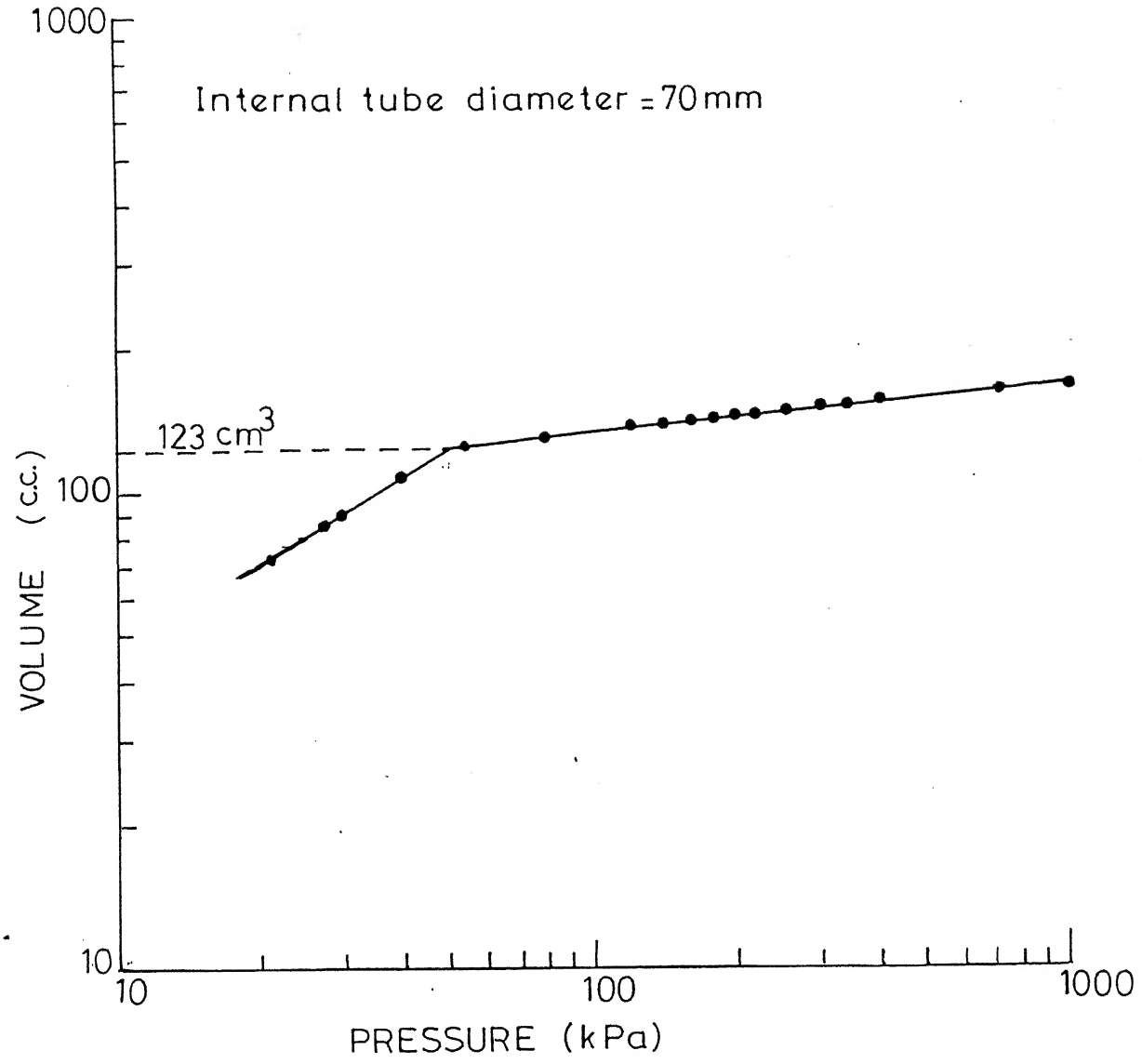


Fig.3·8 Pressure volume calibration curve

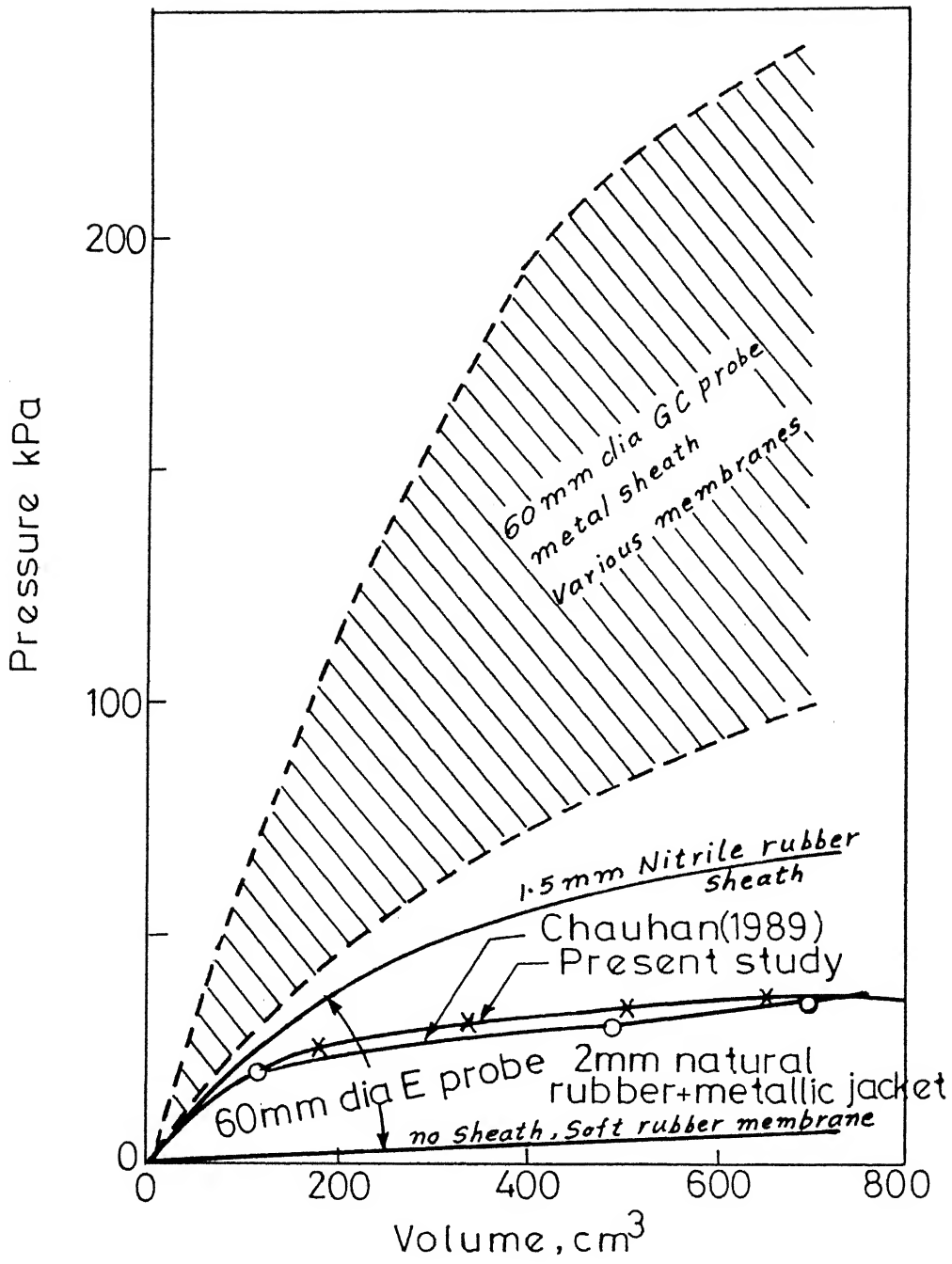


Fig.3·9 Membrane resistance of various probes (After Bageuelin,1978)

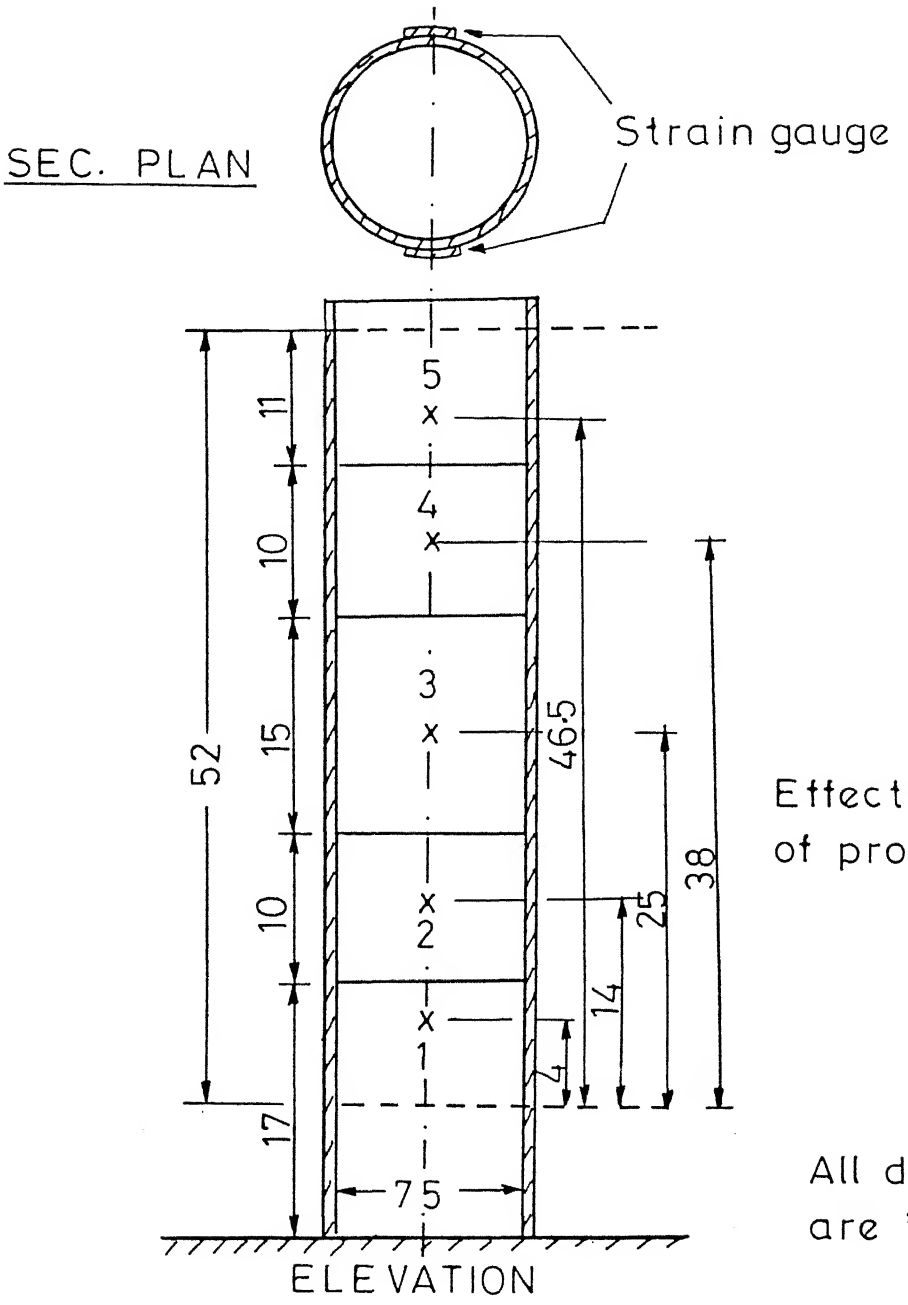


ALUMINIUM TUBE CONSISTED OF A STACK OF FIVE RINGS

x → POSITION OF THE STRAIN GAUGES

FIG. 3.10 STRAIN GAUGE AND RING POSITION FOR IMPROVED CALIBRATION

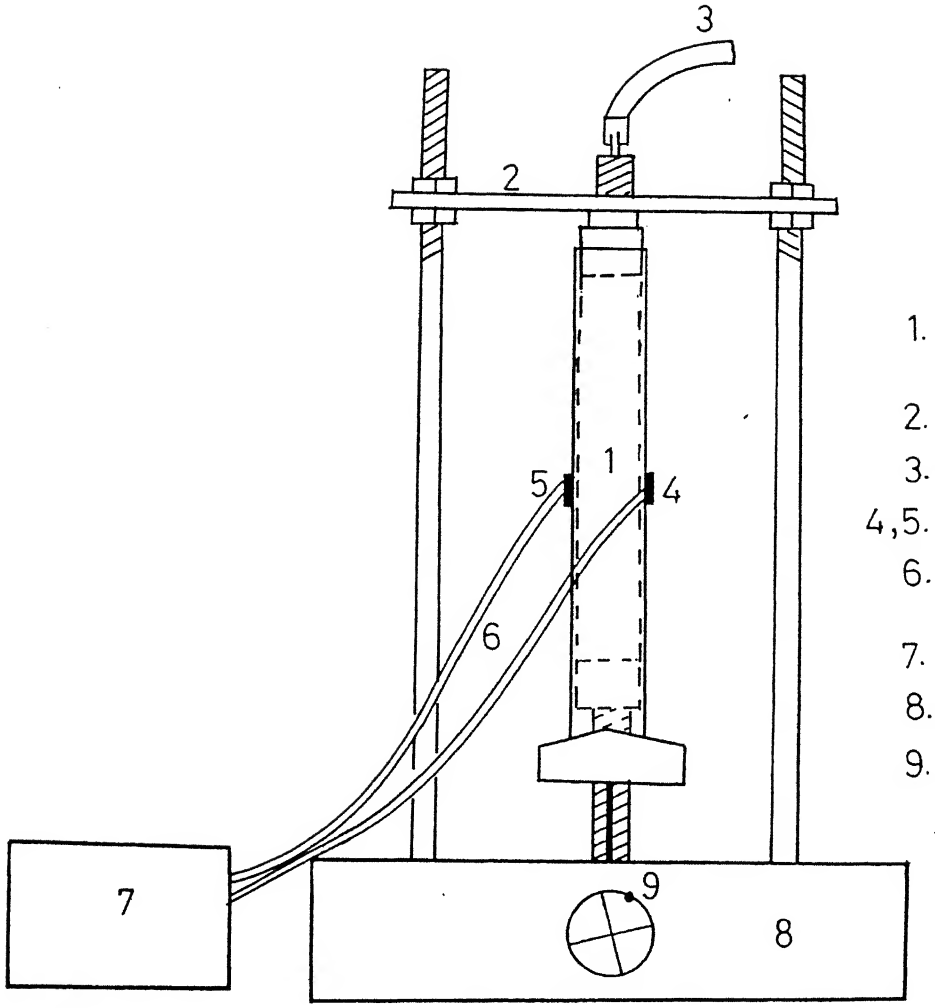


LEGEND

1. Aluminium tube covering the probe
2. Steel plate
3. Connecting tube

4,5. Strain gauge

6. PVC Coated electrical wire
7. Strain indicator
8. Pedestal
9. Handle

FIG. 3·11 EXPERIMENTAL SET-UP FOR IMPROVED CALIBRATION

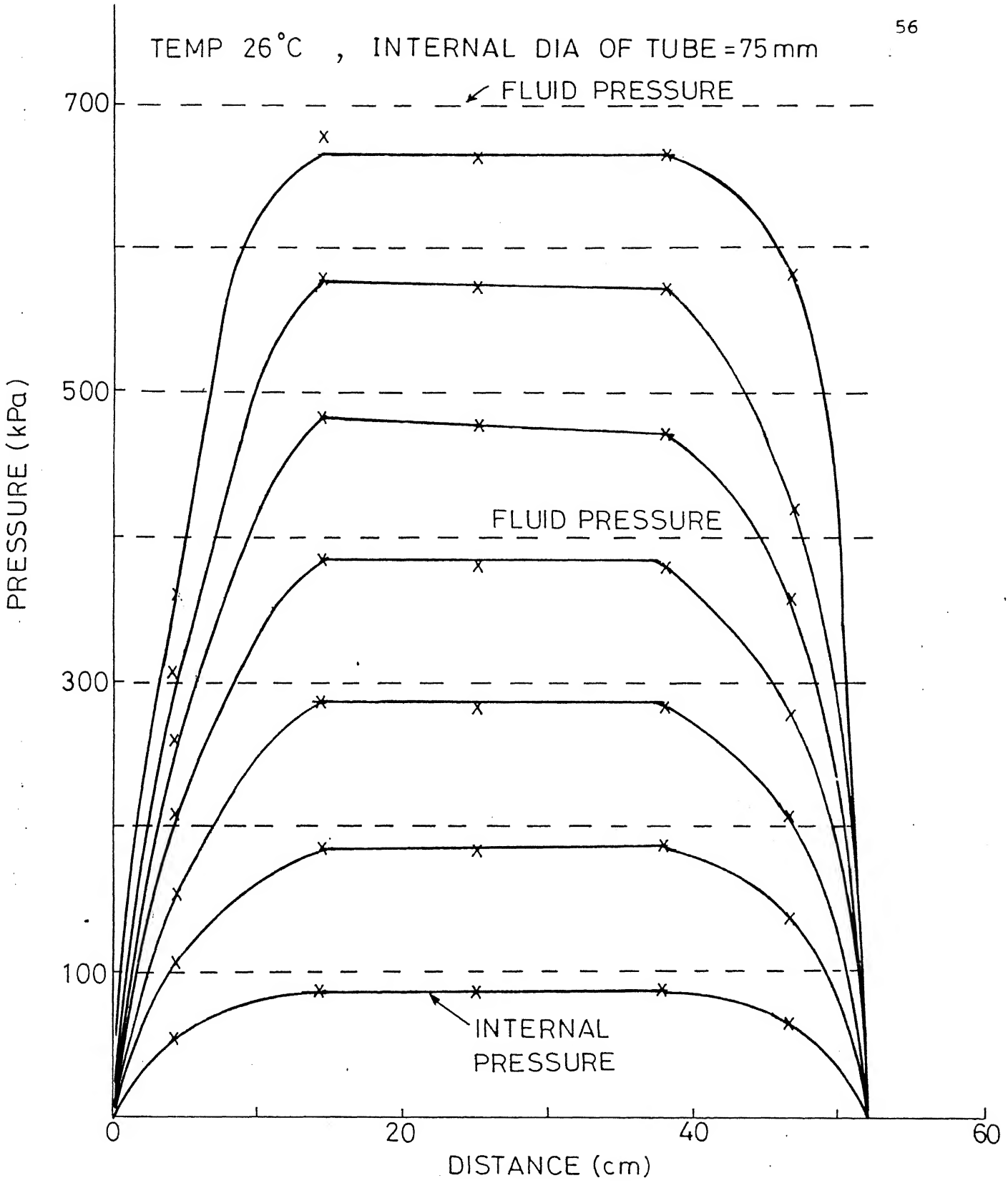


FIG.3·12 PRESSURE DISTRIBUTION ALONG THE PROBE LENGTH

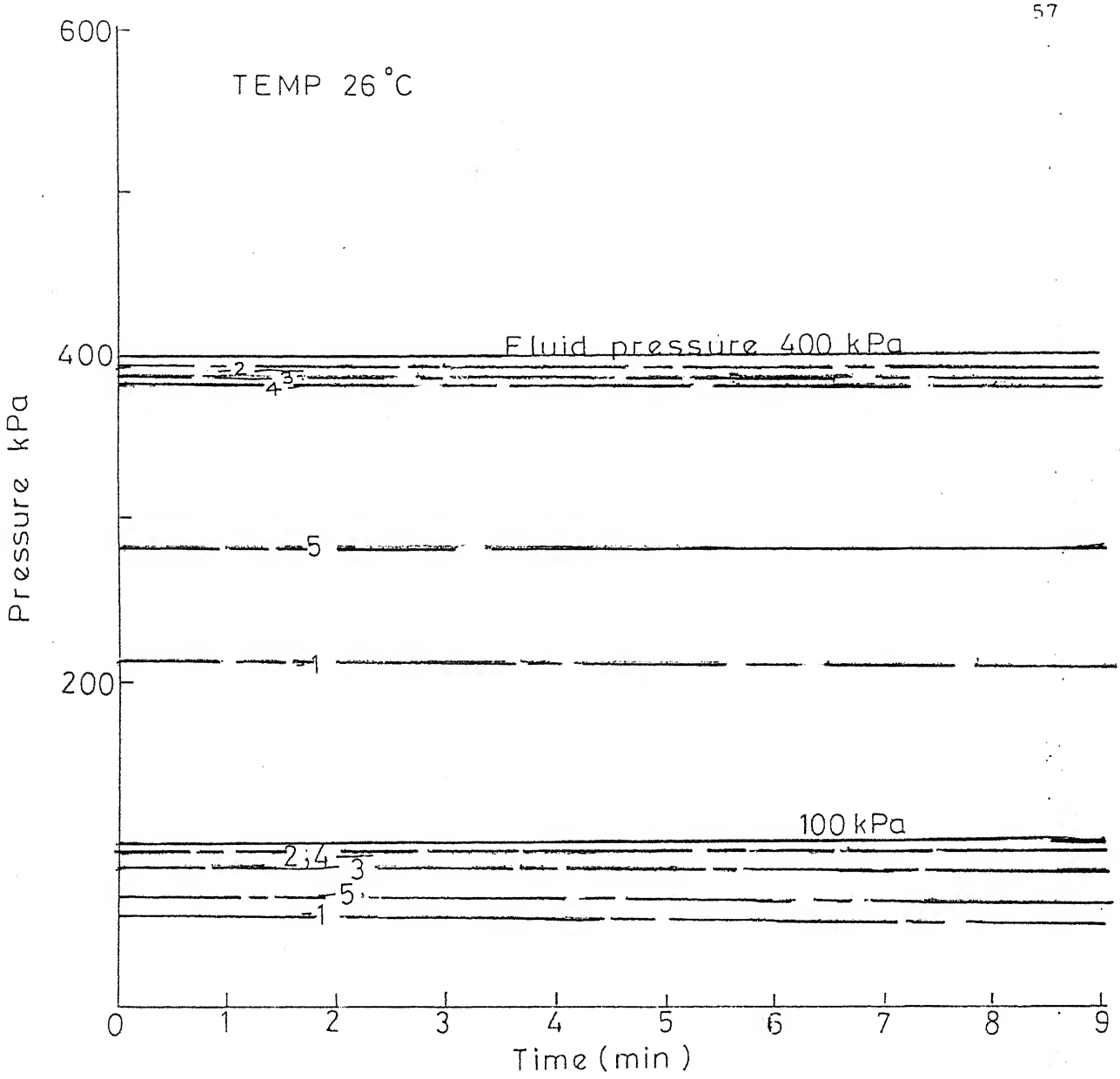


Fig.3·13(a)Evolution of internal pressure with time

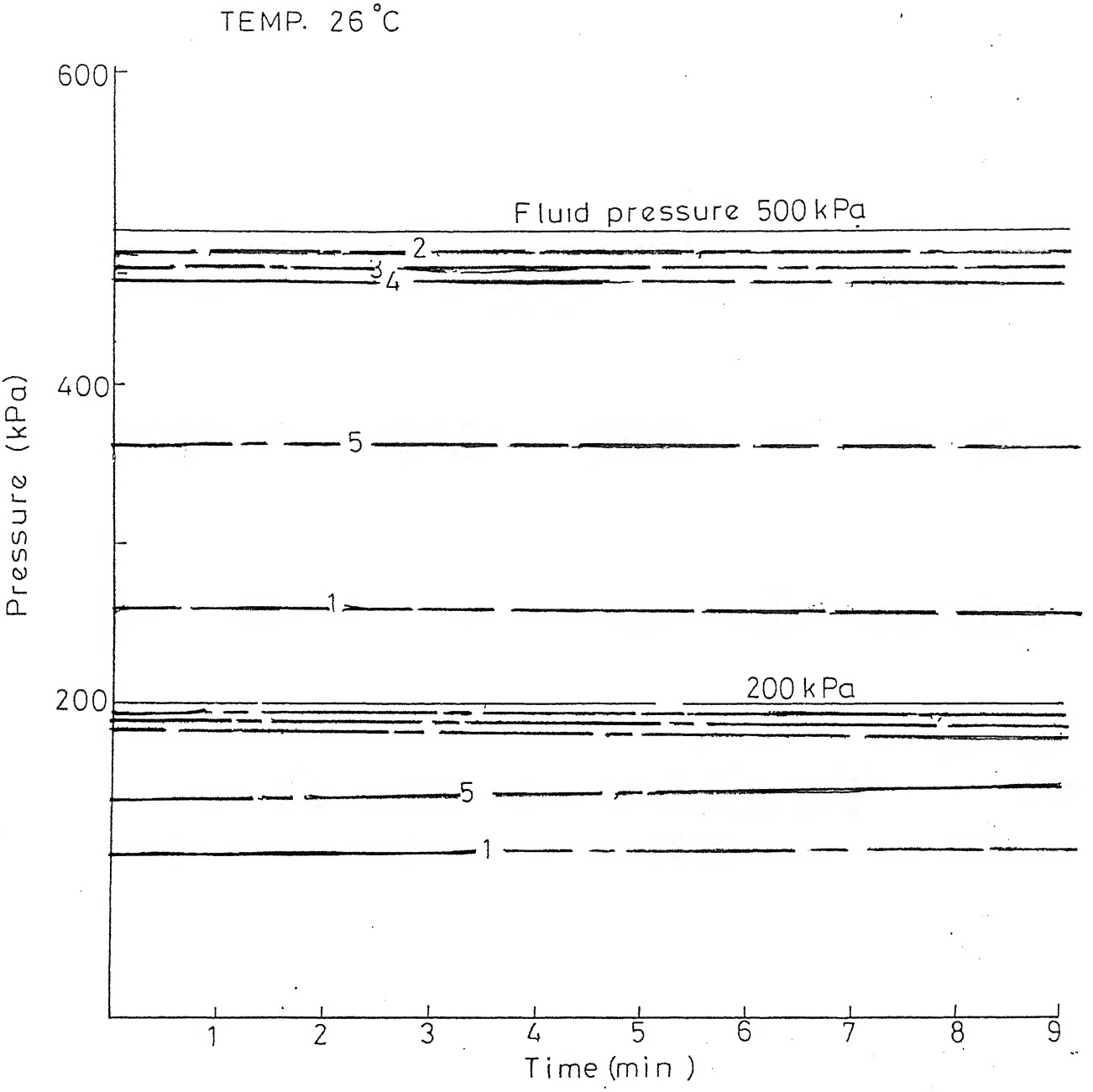


Fig.3.13 (b) Evolution of internal pressure with time

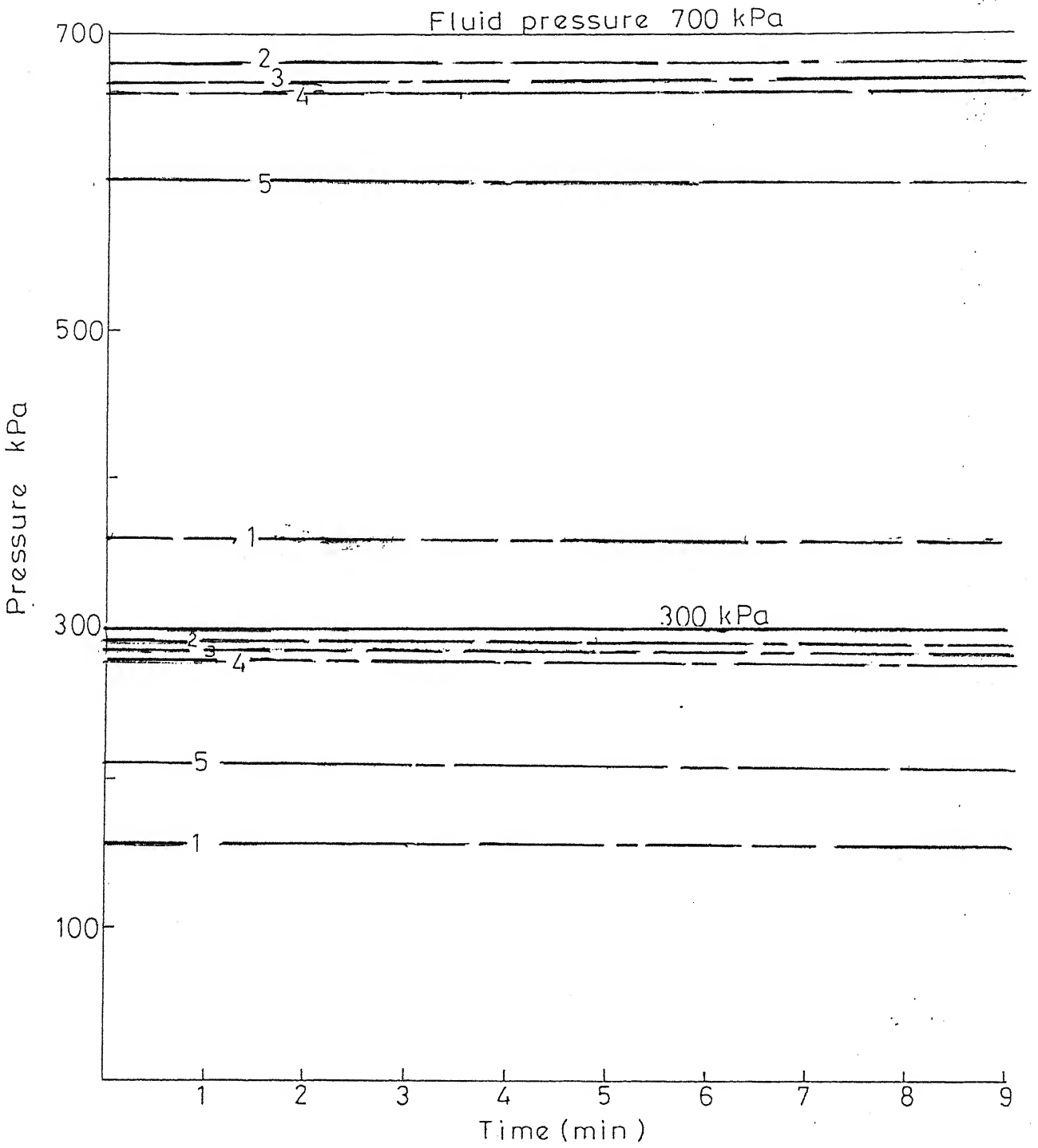


Fig. 3·13(c) Evolution of internal pressure with time

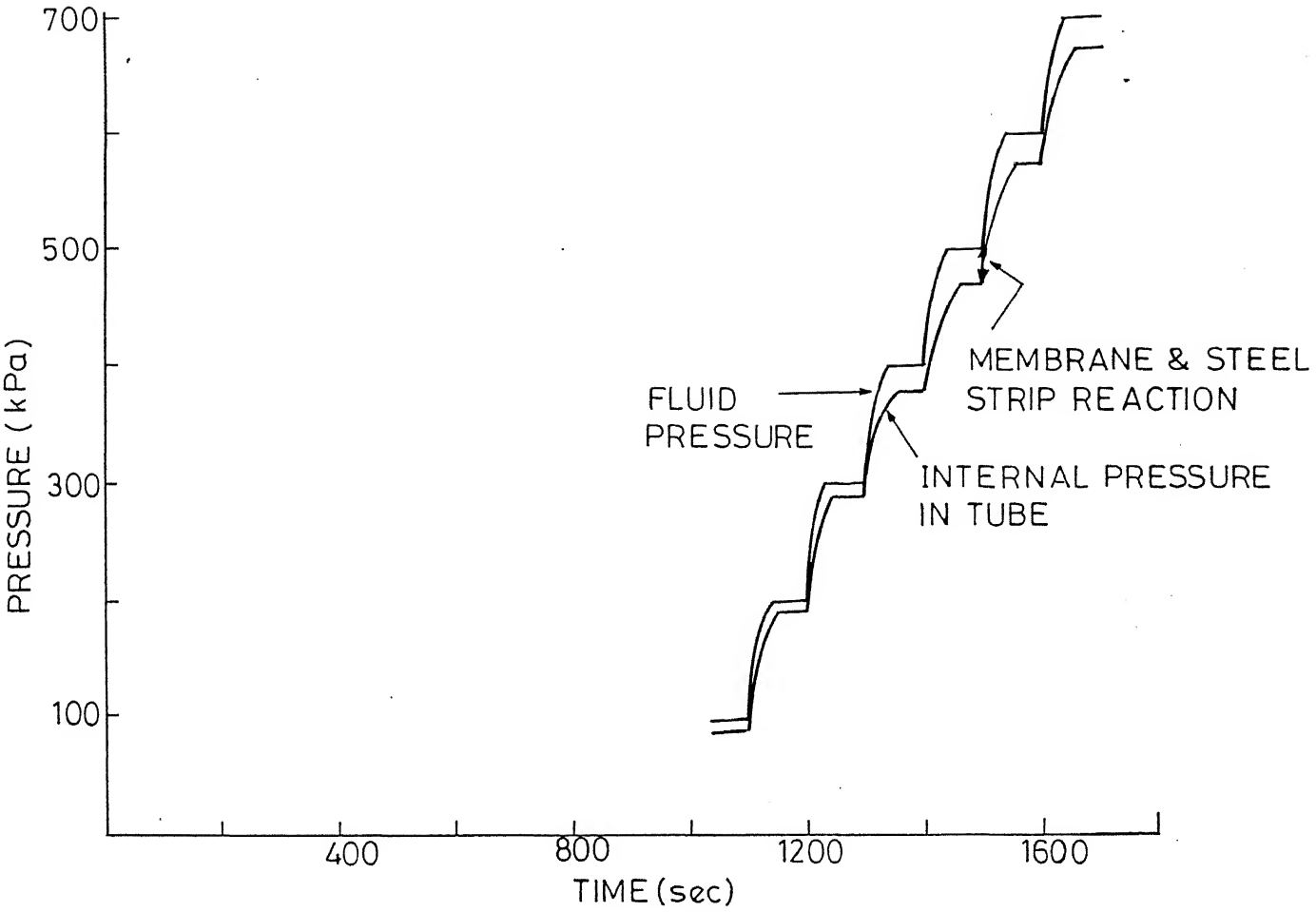


Fig.3·14 Variation of pressure with time: Measurement with single tube

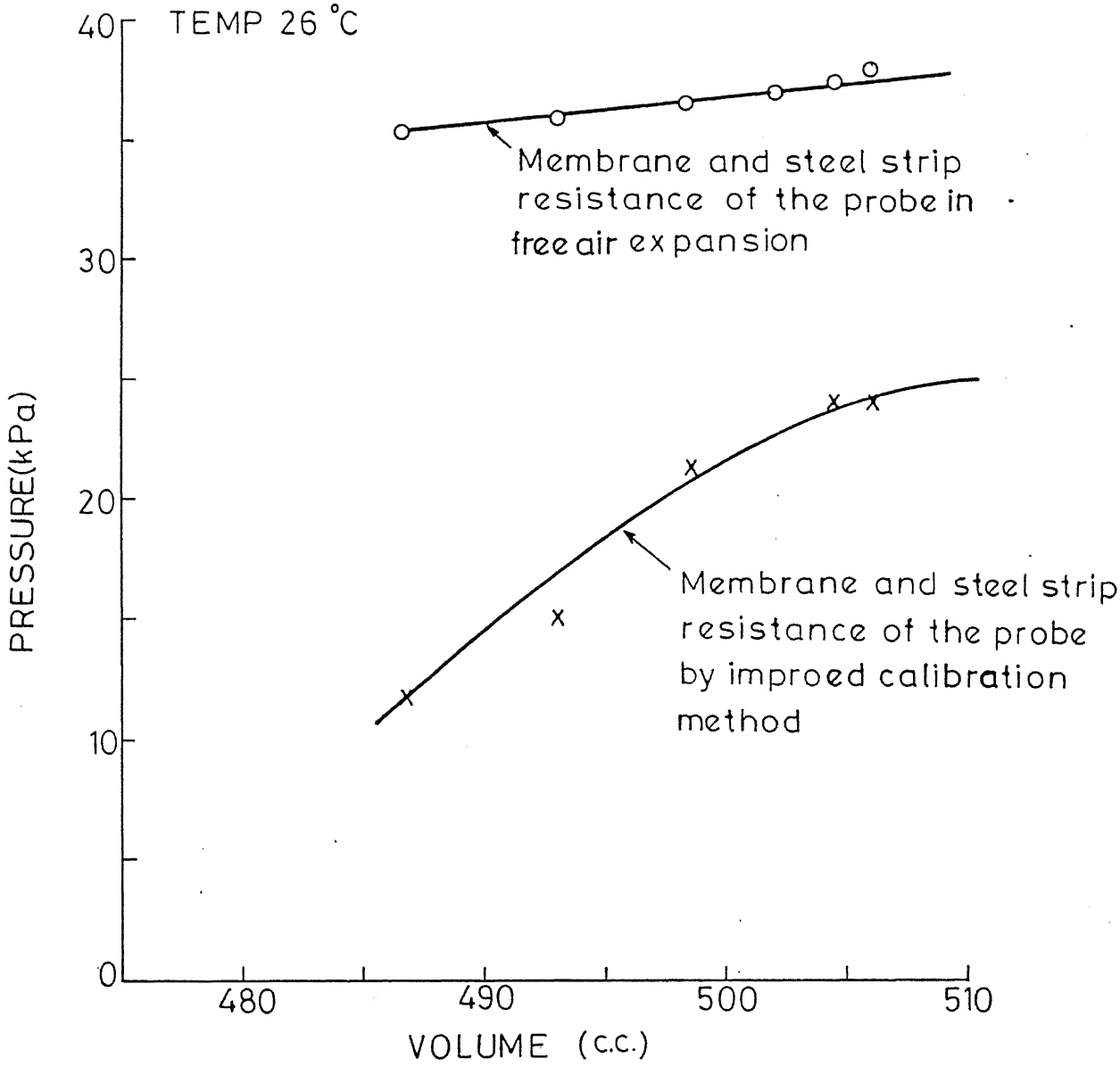


Fig.3·15 Comparison of free air and confined expansion calibration techneques

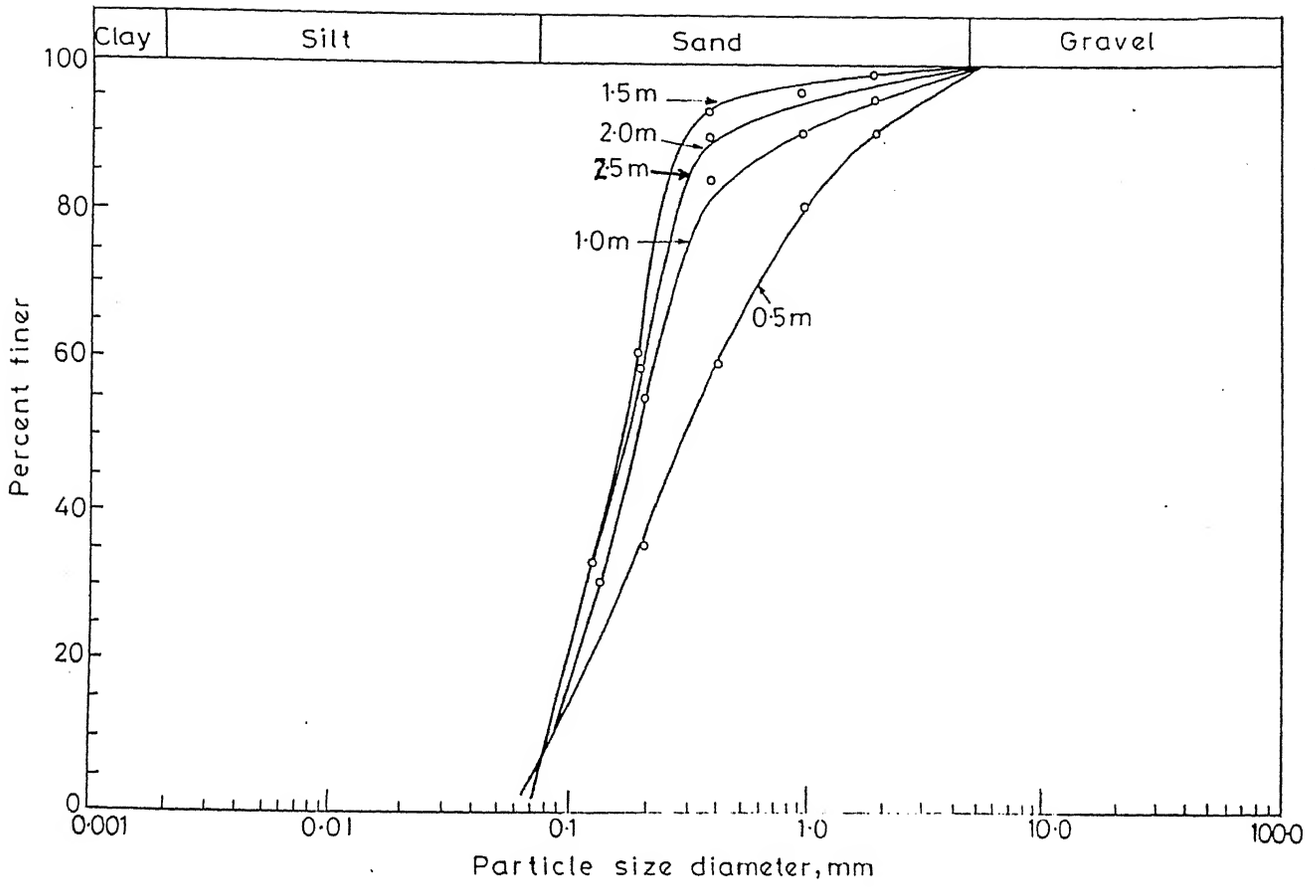


Fig.4·2 Gradation curves for soils

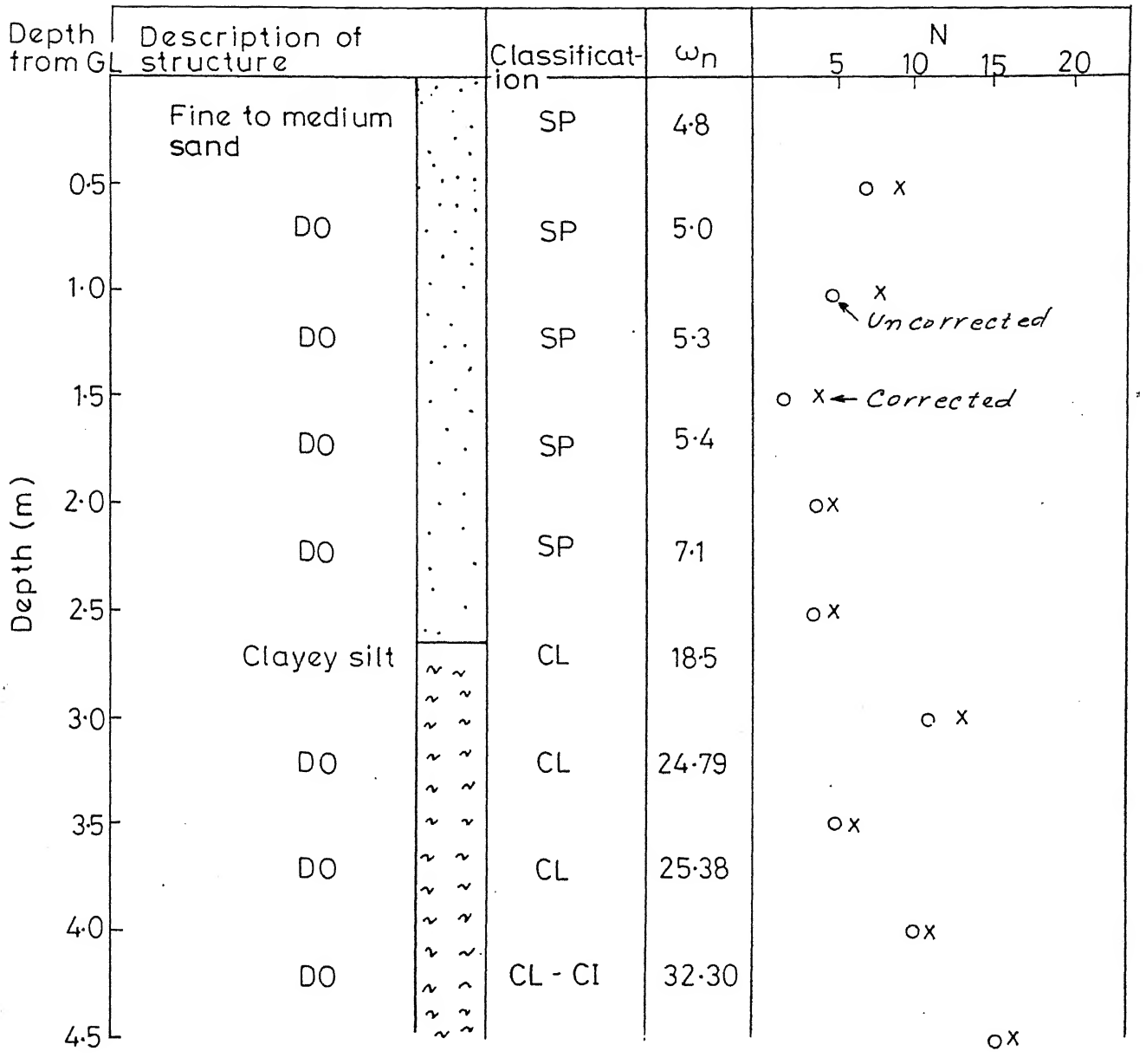


Fig. 4·3 Strata variation with SPT

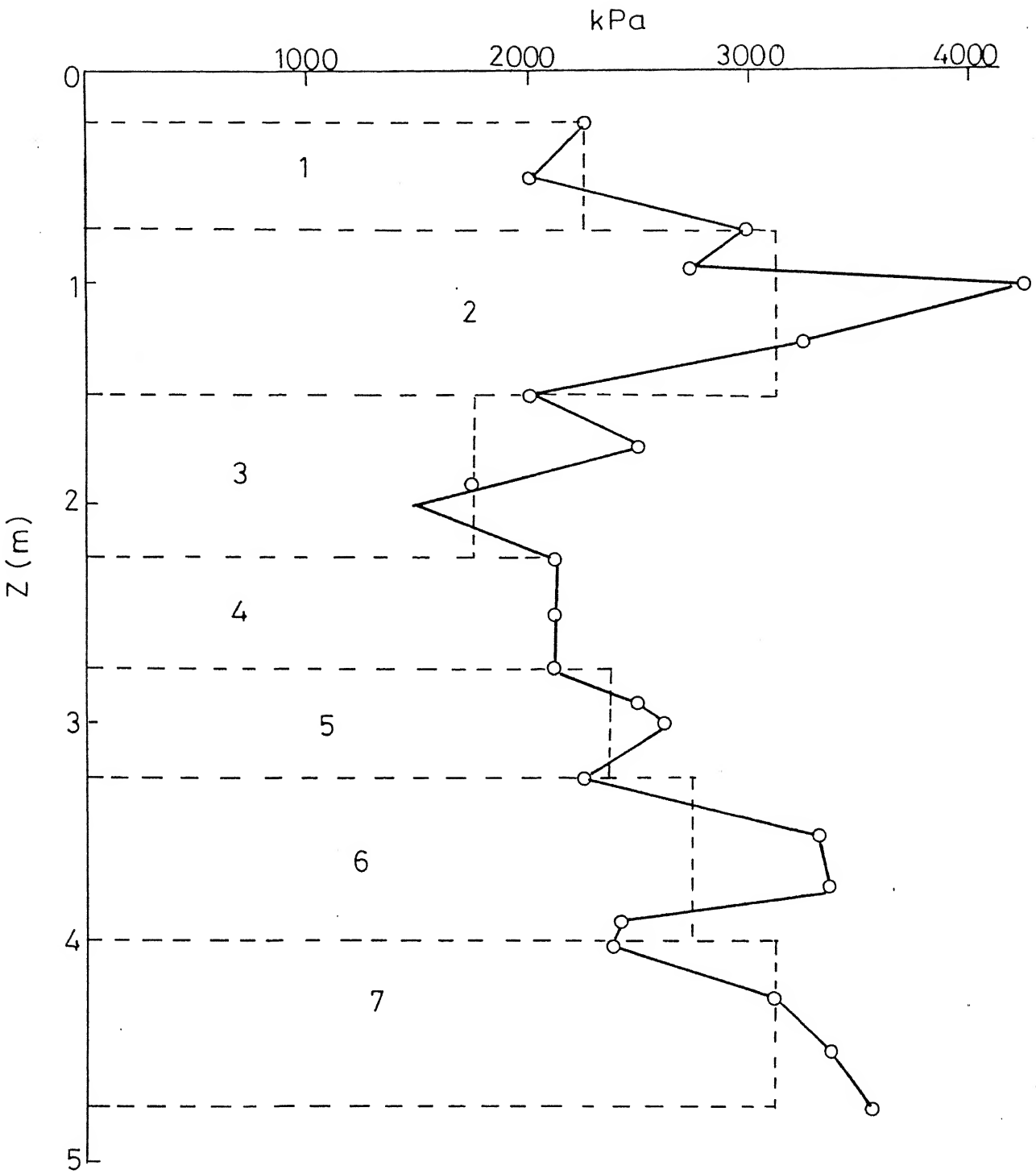


Fig.4·4 Variation of $q_c$ with depth

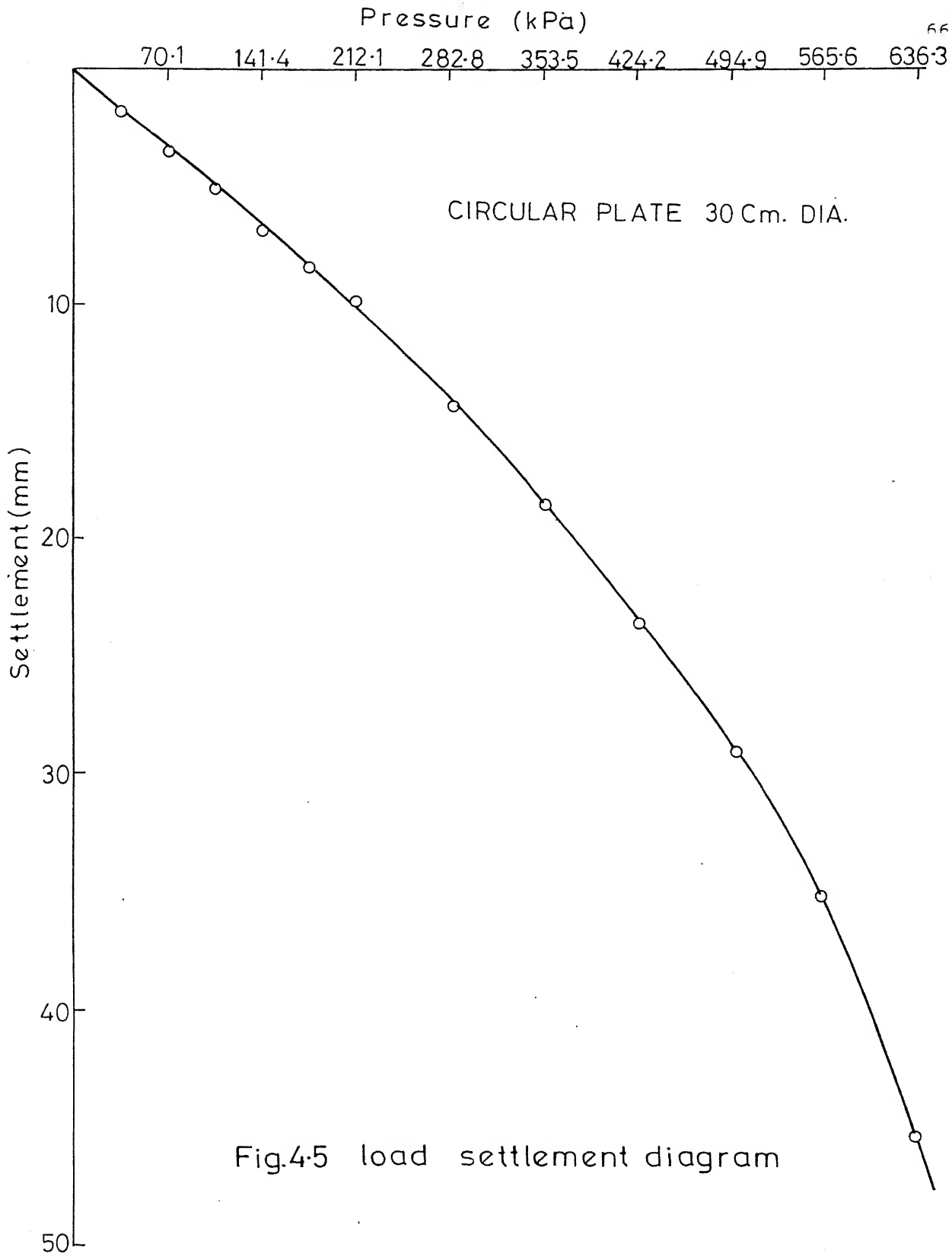


Fig.4·5 load settlement diagram

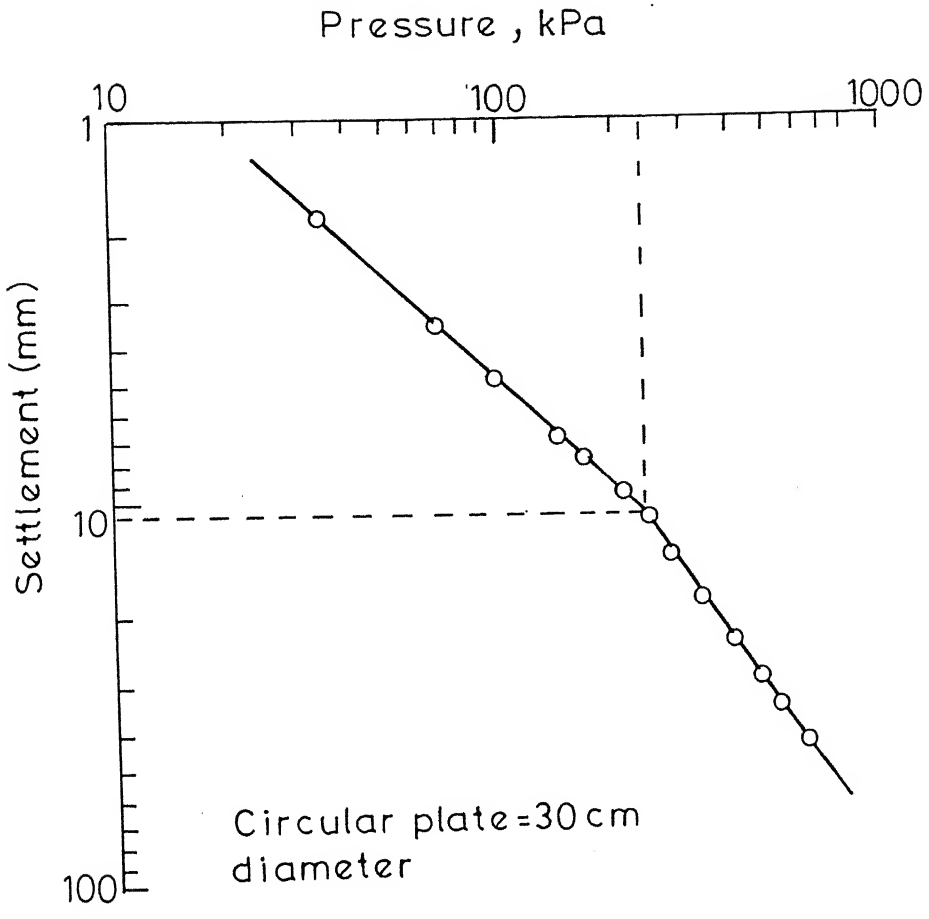


Fig. 4·6 load settlement diagram

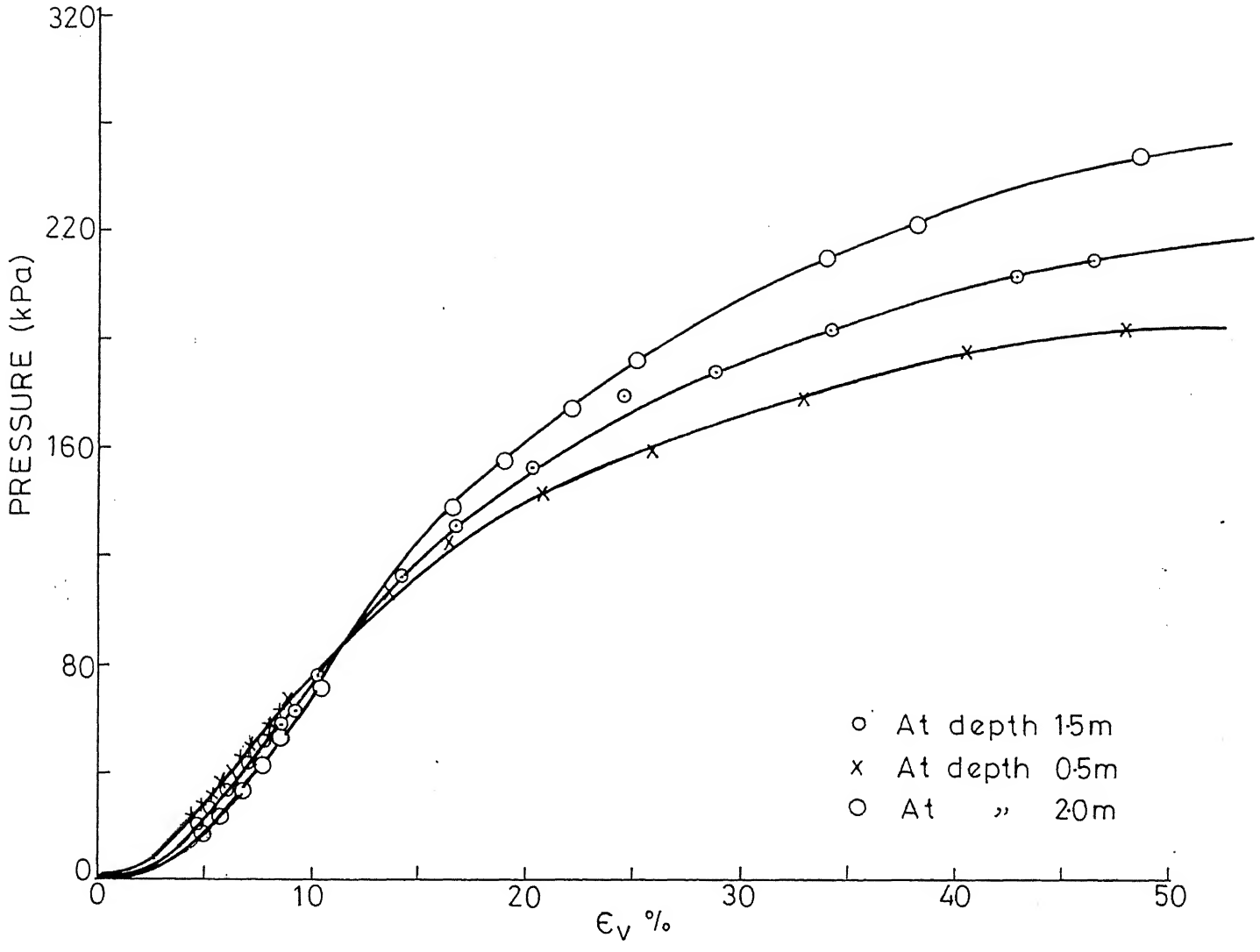


Fig.4·7 Pressure vs. volumetric strain diagram

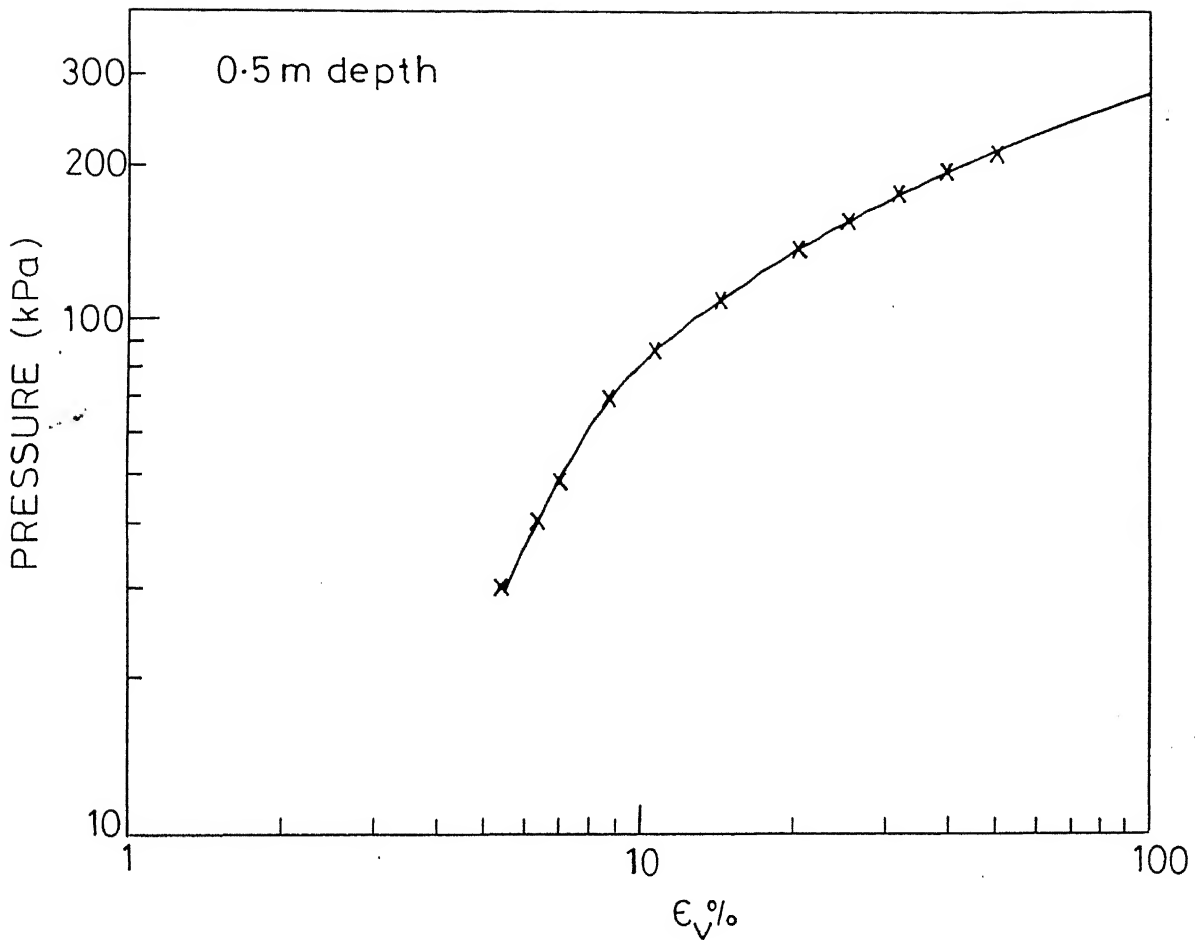


Fig.4·8(a) Pressure vs volumetric strain diagram

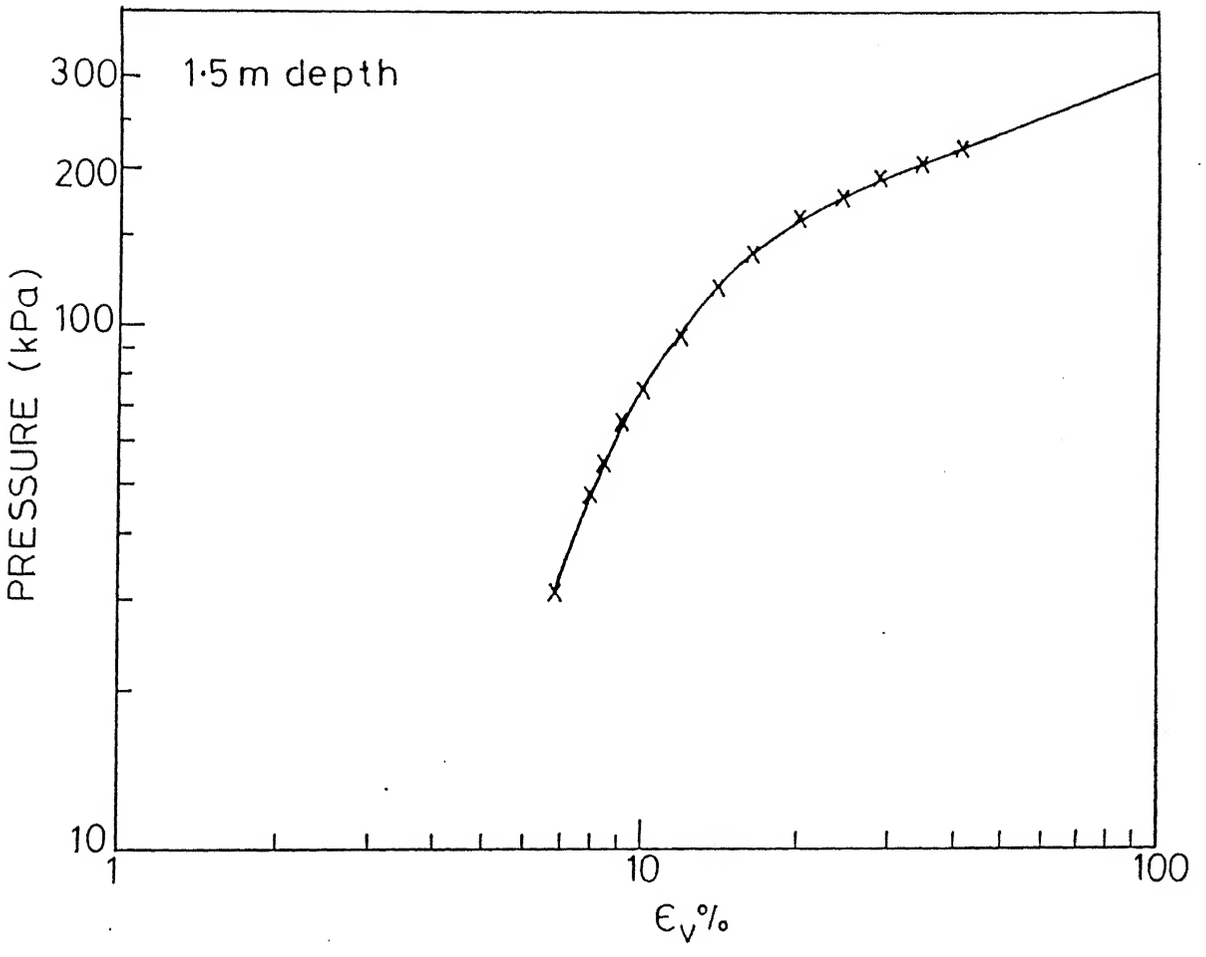


Fig.48(b)Pressure vs volumetric strain diagram

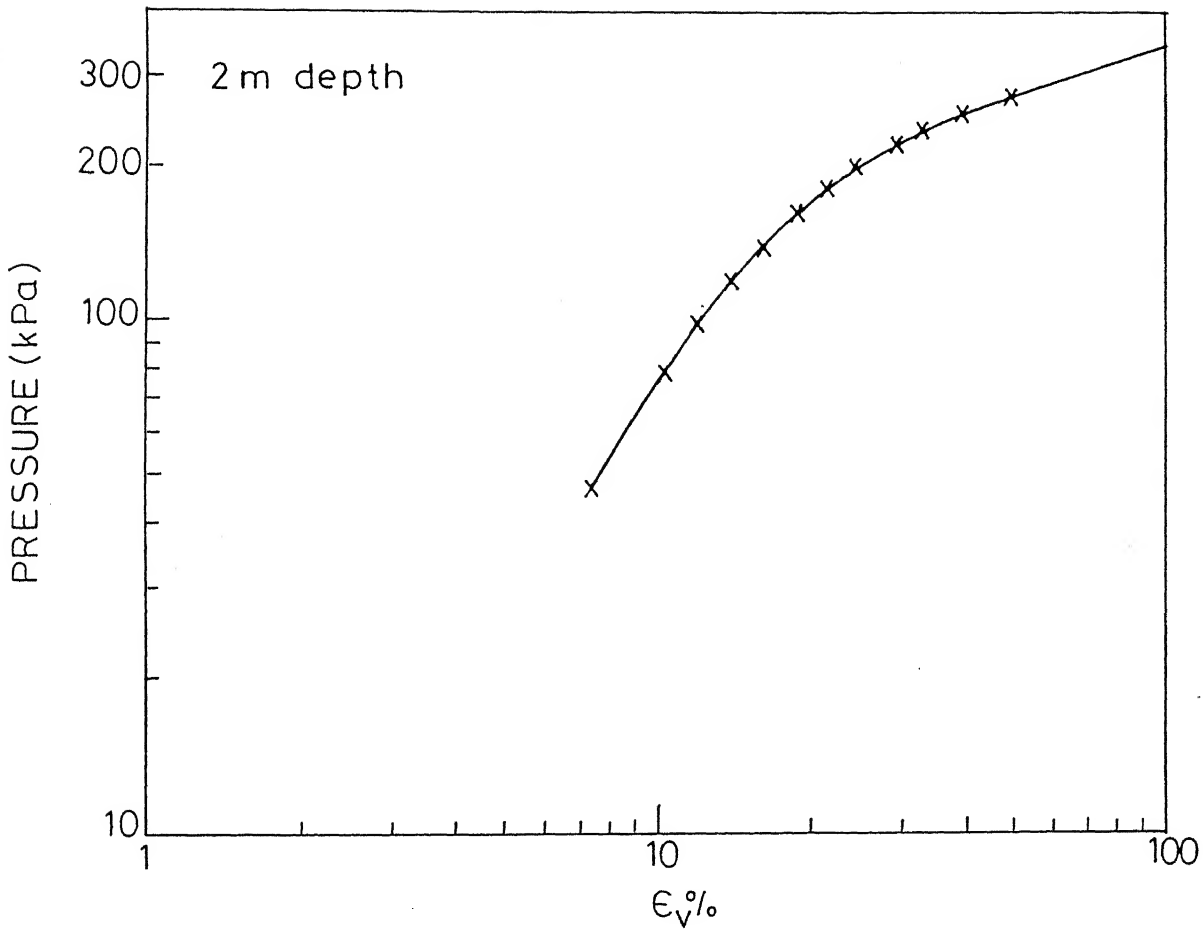


Fig 4.8(c) Pressure vs. volumetric strain diagram

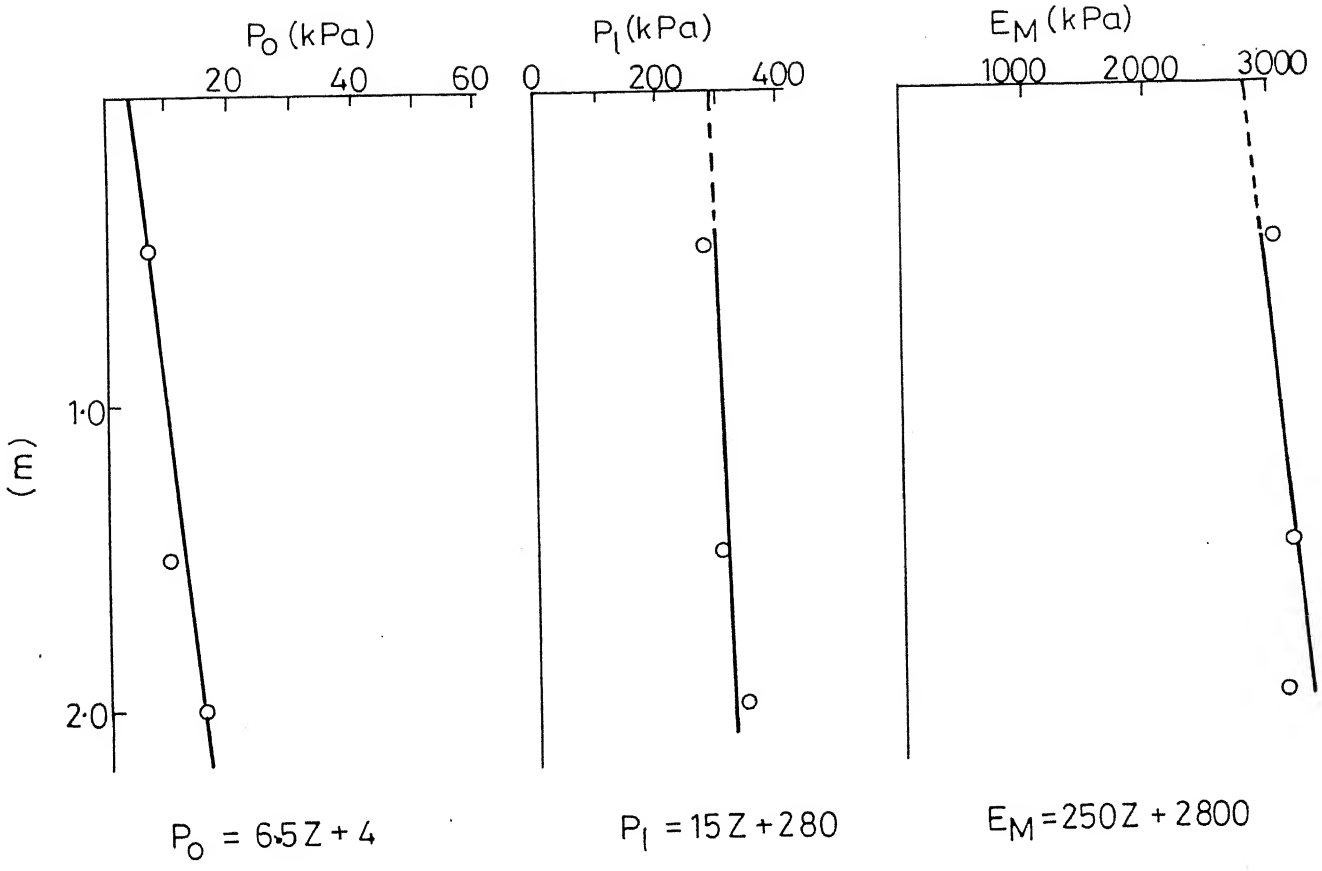


Fig.4·9 Variation of $P_o$ , $P_l$ and $E_M$ with depth

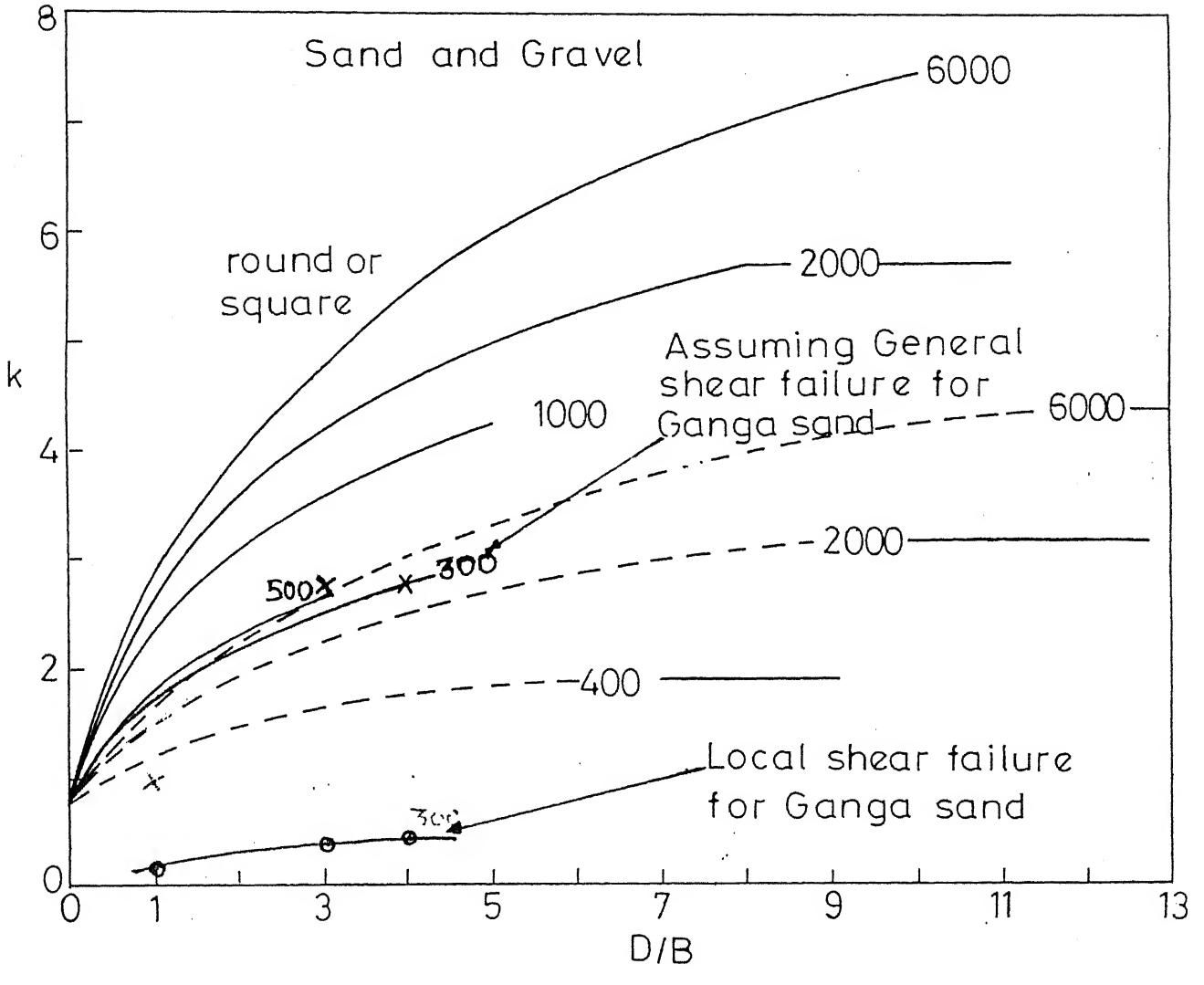


Fig.4·10 k-values for sand and gravel

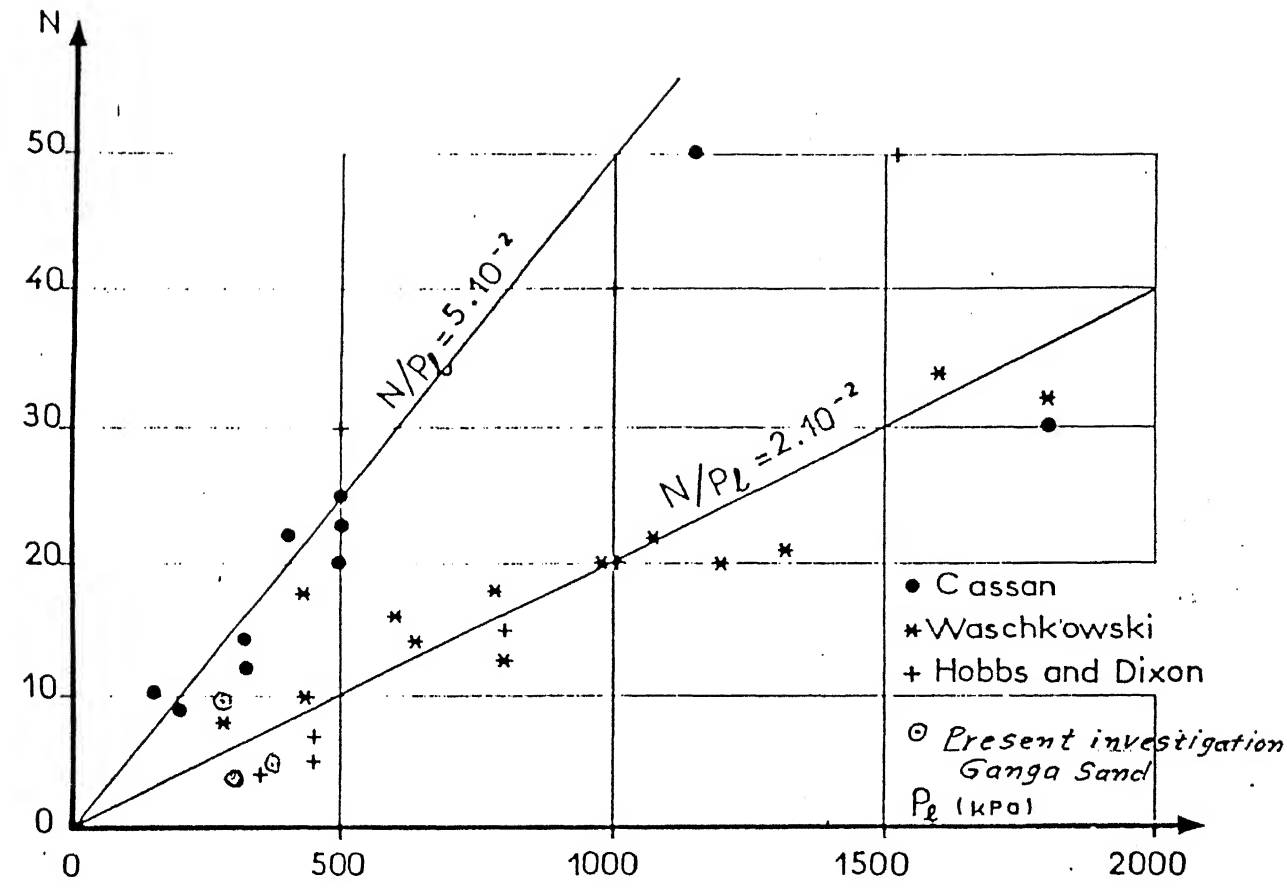


Fig. 4.11 Comparison between $N$ and $p_l$.

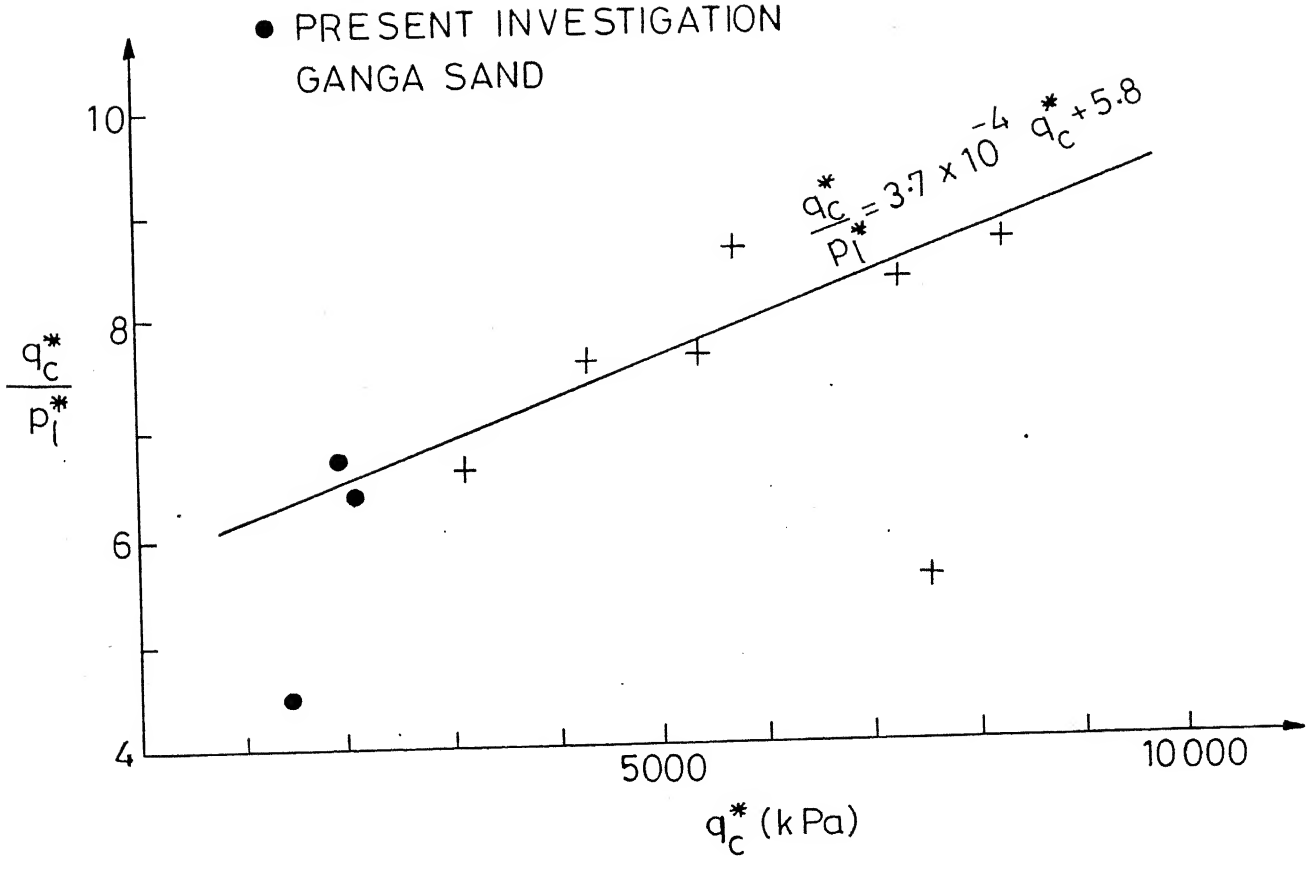


Fig. 4 12 Loire sand Ratio of $q_c^*/p_1^*$ as a function of $q_c^*$ (Ref : Baguelin et.al. (1978),)